

# Optimizing Brownian heat engine with shortcut strategy

Jin-Fu Chen<sup>1,\*</sup>

<sup>1</sup>*School of Physics, Peking University, Beijing, 100871, China*

(Dated: July 18, 2022)

Shortcuts to isothermality provide a powerful method to speed up quasistatic thermodynamic processes within finite-time manipulation. We employ the shortcut strategy to design and optimize Brownian heat engines, and formulate a geometric description of the energetics with the thermodynamic length. We obtain a tight and reachable bound of the output power, which is reached by the optimal protocol to vary the control parameters with a proper constant velocity of the thermodynamic length. Our results generalize the previous optimization in the highly underdamped and the overdamped regimes to the general-damped situation, and are applicable for arbitrary finite-time cycles.

*Introduction.* In the past few decades, the flourishing stochastic thermodynamics has brought great interest in studying the nonequilibrium thermodynamics of microscopic systems featured with fluctuations [1–7]. Down-sized to microscopic systems, the heat engines have been invented with a single trapped ion or a Brownian particle in experiments [8, 9]. Seeking the optimal control schemes of microscopic systems is crucial to designing microscopic machines with high accuracy and low irreversibility. Various methods have been proposed to optimize the control schemes of heat-engine cycles, for example, the optimal control theory to find the optimal configuration of ideal-gas [10, 11] and two-level heat engines [12], and the thermodynamic geometry to optimize slow isothermal processes [13–20]. For Brownian heat engines, the optimal control of the cycle is known in the highly underdamped [21, 22] and the overdamped regimes [23, 24].

Shortcuts to isothermality were recently proposed for the Brownian motion model [25, 26], and experimentally realized with the optical tweezers [27–29]. By implementing an auxiliary Hamiltonian, the system is steered to evolve along instantaneous equilibrium states of the original Hamiltonian within finite-time manipulation. Such a strategy is feasible to speed up heat-engine cycles [30–32] and the control of biophysical processes [33, 34]. In addition, the temperature can also be treated as a time-dependent control parameter according to the generalization in Refs. [35, 36]. In the shortcut strategy, the thermodynamic cost, as the irreversible work  $W_{\text{irr}}$  to implement the auxiliary Hamiltonian, is bounded by the thermodynamic length  $\mathcal{L}$  as [36, 37]

$$W_{\text{irr}} \geq \mathcal{L}^2/\tau, \quad (1)$$

It is remarkable that this bound holds for arbitrary finite-time shortcut processes. The equality is saturated by the optimal protocol to vary the control parameters with a constant velocity of the thermodynamic length [37].

In this Letter, we analyze the thermodynamic cost of shortcut processes with both work parameter and temperature time-dependent, and formulate a geometric description of the energetics based on the thermodynamic

length. Previous studies of thermodynamic length associated with the corresponding optimization are usually limited to the slow-driving regime [13–20, 38–48]. Our setup does not have this limitation. We employ the shortcut strategy to design and optimize the Brownian heat engine in the general-damped situation, and derive the maximum power and the efficiency at the maximum power (EMP) expressed by the thermodynamic length. We also obtain the optimal protocol of the cycle to reach the maximum power.

*Setup.* We consider a heat engine with a single Brownian particle as the working substance. The probability distribution  $\rho = \rho(x, p, t)$  for the Brownian particle evolves according to the complete Fokker-Planck equation (the Kramer equation) [49]

$$\frac{\partial \rho}{\partial t} = \mathcal{L}[\rho] + \mathcal{D}[\rho], \quad (2)$$

where  $\mathcal{L}[\rho] = -\partial_x(\rho\partial_p H) + \partial_p(\rho\partial_x H)$  and  $\mathcal{D}[\rho] = \kappa m \partial_p(\rho\partial_p H + \partial_p \rho/\beta)$  reflect the deterministic and the dissipative parts of the evolution with the total Hamiltonian  $H$ , the mass  $m$  of the particle, the friction coefficient  $\kappa$ , and the inverse temperature  $\beta$  of the environment.

In the shortcut strategy [26], the total Hamiltonian is  $H = H_o + H_a$ . An auxiliary Hamiltonian  $H_a(x, p, t)$  is implemented to steer the system evolving along instantaneous equilibrium states  $\rho_{\text{ieq}} := \exp\{\beta[F(\lambda, \beta) - H_o(x, p, \lambda)]\}$  of the original Hamiltonian  $H_o(x, p, \lambda) = p^2/(2m) + U_o(x, \lambda)$  with the potential  $U_o(x, \lambda)$  and the work parameter  $\lambda$ . The free energy  $F(\lambda, \beta)$  is determined by  $\beta F(\lambda, \beta) = -\ln\{\iint \exp[-\beta H_o(x, p, \lambda)] dx dp\}$ . The auxiliary Hamiltonian is solved in the form  $H_a(x, p, t) = \dot{\lambda} h_\lambda(x, p, \lambda) + \dot{\beta} h_\beta(x, p, \lambda, \beta)$ , where  $h_\lambda(x, p, \lambda)$  and  $h_\beta(x, p, \lambda, \beta)$  are two auxiliary functions related to the original Hamiltonian [26, 35, 50].

We employ the shortcut strategy to construct a heat-engine cycle. The work parameter  $\lambda$  and the inverse temperature  $\beta$  are time-dependent control parameters, and are cyclical functions of the operation time. The input power and the heat flux are defined as  $\dot{W} := \langle \partial_t H \rangle$  and  $\dot{Q} := \iint H \partial_t \rho_{\text{ieq}} dx dp$  [1], where the average is over an in-

stantaneous equilibrium state  $\langle \cdot \rangle := \iint (\cdot) \rho_{\text{ieq}} dx dp$ . Positive  $\dot{W}$  and  $\dot{Q}$  indicate the work is performed on the system and the heat is absorbed by the system from the environment, respectively. We divide  $\dot{W}$  and  $\dot{Q}$  into the quasistatic and the irreversible parts

$$\dot{W} = \dot{W}_o + \dot{W}_{\text{irr}}, \quad (3)$$

$$\dot{Q} = \dot{Q}_o + \dot{Q}_{\text{irr}}, \quad (4)$$

according to  $H_o$  and  $H_a$ . The quasistatic and the irreversible input powers are  $\dot{W}_o = \dot{\lambda} \langle \partial_\lambda H_o \rangle$  and  $\dot{W}_{\text{irr}} = \langle \partial_t H_a \rangle$ . The quasistatic and the irreversible heat fluxes are  $\dot{Q}_o = \iint H_o \partial_t \rho_{\text{ieq}} dx dp$  and  $\dot{Q}_{\text{irr}} = \iint H_a \partial_t \rho_{\text{ieq}} dx dp$ . The first law of thermodynamics is satisfied for each part  $\partial_t \langle H_o \rangle = \dot{W}_o + \dot{Q}_o$  and  $\partial_t \langle H_a \rangle = \dot{W}_{\text{irr}} + \dot{Q}_{\text{irr}}$ . In isothermal processes ( $\beta(t) \equiv \beta$ ), the quasistatic work is equal to the free energy change  $W_o = F(\lambda(\tau), \beta) - F(\lambda(0), \beta)$  [26]. In general shortcut processes with both  $\lambda(t)$  and  $\beta(t)$  time-dependent, the quasistatic work  $W_o = \int \lambda'(s) \langle \partial_\lambda H_o \rangle ds$  relies on the path  $(\lambda(s), \beta(s))$  in the control-parameter space, but is independent of the protocol and the operation time. The irreversible heat is carried out as [50]

$$Q_{\text{irr}} = - \int_0^\tau (\dot{\lambda} \ \dot{\beta}) \mathbf{g} \begin{pmatrix} \dot{\lambda} \\ \dot{\beta} \end{pmatrix} dt, \quad (5)$$

with the metric

$$\mathbf{g} = \kappa m \begin{pmatrix} \left\langle \frac{\partial h_\lambda}{\partial p} \frac{\partial h_\lambda}{\partial p} \right\rangle & \left\langle \frac{\partial h_\lambda}{\partial p} \frac{\partial h_\beta}{\partial p} \right\rangle \\ \left\langle \frac{\partial h_\lambda}{\partial p} \frac{\partial h_\beta}{\partial p} \right\rangle & \left\langle \frac{\partial h_\beta}{\partial p} \frac{\partial h_\beta}{\partial p} \right\rangle \end{pmatrix}. \quad (6)$$

The irreversible work is

$$W_{\text{irr}} = \langle H_a \rangle (\tau^+) - \langle H_a \rangle (0^-) - Q_{\text{irr}}, \quad (7)$$

where  $0^-$  and  $\tau^+$  denote the initial time and the final time of the shortcut process. The auxiliary Hamiltonian  $H_a$  is switched on at the beginning and off at the end of the shortcut process, and thus  $\langle H_a \rangle (\tau^+) - \langle H_a \rangle (0^-) = 0$ . This term also vanishes in a heat-engine cycle due to the cyclical variation of the control parameters. The metric  $\mathbf{g}$  is positive semi-definite [50]. Therefore, the irreversible work is non-negative  $W_{\text{irr}} \geq 0$ . For a given path  $(\lambda(s), \beta(s))$  in the control-parameter space, the thermodynamic length is defined as

$$\mathcal{L} := \int \sqrt{(\lambda'(s) \ \beta'(s)) \mathbf{g} \begin{pmatrix} \lambda'(s) \\ \beta'(s) \end{pmatrix}} ds, \quad (8)$$

which provides a tight and reachable bound (1) of the irreversible work in general shortcut processes.

By applying the bound (1) to a heat-engine cycle, the output power  $P := -W/\tau$  is bounded by  $P \leq -W_o/\tau - \mathcal{L}^2/\tau^2$ . The equality is saturated with the optimal protocol, and the irreversible heat flux becomes a negative constant during the whole cycle

$$\dot{Q}_{\text{irr}} \equiv -\frac{\mathcal{L}^2}{\tau^2}. \quad (9)$$

By further choosing the operation time  $\tau = \tau_{\text{max}} := 2\mathcal{L}^2/(-W_o)$ , the maximum power is reached

$$P_{\text{max}} = \frac{(-W_o)^2}{4\mathcal{L}^2}. \quad (10)$$

Further optimization of the output power of the cycle is converted to finding out the closed path with a large ratio  $-W_o/\mathcal{L}$ .

According to positive (negative) quasistatic heat flux  $\dot{Q}_o > 0$  ( $\dot{Q}_o < 0$ ), we divide the cycle into the heat absorbed (released) path with the thermodynamic length  $\mathcal{L}_+$  ( $\mathcal{L}_-$ ) satisfying  $\mathcal{L} = \mathcal{L}_+ + \mathcal{L}_-$ . The overall heat absorbed (released) on each path is  $Q_+ = Q_{o,+} + Q_{\text{irr},+}$  ( $Q_- = Q_{o,-} + Q_{\text{irr},-}$ ). The efficiency of the cycle is defined as  $\eta := -W/Q_+$ . In the optimal protocol, the overall heat absorbed is explicitly  $Q_+ = Q_{o,+} - \mathcal{L}_+\mathcal{L}/\tau$ . The variation of the temperature is constrained between the lowest  $T_L$  and the highest temperatures  $T_H$ . At the maximum power, the efficiency is expressed by the thermodynamic length as [50]

$$\eta_{\text{EMP}} = \frac{\eta_o}{2 - \eta_o \mathcal{L}_+/\mathcal{L}}, \quad (11)$$

where  $\eta_o := -W_o/Q_{o,+}$  is the efficiency of the quasistatic cycle and is less than the Carnot efficiency  $\eta_C := 1 - T_L/T_H$ . We also obtain the maximum power  $P_\eta$  at given efficiency  $\eta$  as [50]

$$\frac{P_\eta}{P_{\text{max}}} = \frac{4(\eta_o - \eta)(1 - \eta_o \mathcal{L}_+/\mathcal{L})\eta}{\eta_o^2(1 - \eta \mathcal{L}_+/\mathcal{L})^2}. \quad (12)$$

Equations (10)-(12) are the main result of this work, and the detailed derivations are left in [50].

*Application to power-law potentials.* We next realize the Brownian heat engine with the shortcut strategy in a class of power-law potentials  $U_o(x, \lambda) = m\lambda^{n+1}x^{2n}/(2n)$  [51], where  $n$  and  $\lambda$  characterize the shape and the stiffness of the potential. The auxiliary Hamiltonian  $H_a$  for these potentials has been derived in Ref. [35], with the auxiliary functions

$$h_\lambda = \frac{f_n}{4\kappa\lambda m} (p - \kappa m x)^2 + \frac{f_n m}{4\kappa n} \lambda^n x^{2n}, \quad (13)$$

$$h_\beta = \frac{\eta p^2 + (p - \kappa m x)^2 + m^2 f_n \lambda^{n+1} x^{2n}}{4\beta \kappa m n}, \quad (14)$$

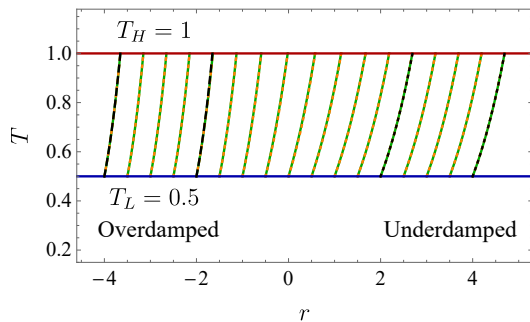


Figure 1. The  $r - T$  diagram with the harmonic potential  $n = 1$ . We set the parameters  $\lambda_0 = 1$ ,  $m = 1$ ,  $\kappa = 1$ , and the temperatures  $T_L = 0.5$  and  $T_H = 1$ , and use these values in all the later discussions. The shortest geodesic path (green solid curves) and the shortest exponential path (orange dashed curves) almost coincide. We also show the zero-length paths  $\alpha = 1$  (black dotted curve) and  $\alpha = n + 1$  (black dashed curve) in the highly underdamped and the overdamped regimes.

where  $f_n = 1 + 1/n$  is the effective degree of freedom [19].

We use a dimensionless work parameter  $r = \ln(\lambda/\lambda_0)$  and the temperature  $T = 1/\beta$  to represent the control parameters, and choose a closed path for the cycle. The quasistatic output work is obtained as  $-W_o = -(f_n/2) \oint T dr$ , which is proportional to the area  $\mathcal{A} = |\oint T dr|$  of the closed path. The thermodynamic length of the cycle is

$$\mathcal{L} = \frac{f_n}{2} \oint \sqrt{\frac{(T dr - dT)^2}{\kappa T} + \frac{\chi}{\kappa T} \left( T dr - \frac{dT}{n+1} \right)^2}, \quad (15)$$

where  $\chi$  is a dimensionless quantity depending on the control parameters

$$\chi = \frac{R_n \kappa^2}{\lambda_0^{f_n} e^{f_n r}} \left( \frac{m}{T} \right)^{1-1/n}, \quad (16)$$

and  $R_n = (2n)^{1/n} \Gamma(3/(2n)) / \Gamma(1/(2n))$  is a pure number ranging from  $1/3$  (reached by  $n \rightarrow \infty$ ) to  $1$  (reached by  $n = 1$ ).  $\Gamma(\cdot)$  is the gamma function. The highly underdamped and the overdamped regimes are reflected by  $\chi \ll 1$  and  $\chi \gg 1$ , respectively. The maximum power (10) is explicitly

$$P_{\max} = \frac{f_n^2 \mathcal{A}^2}{16 \mathcal{L}^2}, \quad (17)$$

with the operation time  $\tau_{\max} = 4\mathcal{L}^2/(f_n \mathcal{A})$ . The area  $\mathcal{A}$  and the thermodynamic length  $\mathcal{L}$  of the closed path are obtained geometrically in the  $r - T$  diagram.

To construct a cycle, we pick up four boundary points  $(r_1, T_L)$ ,  $(r_2, T_L)$ ,  $(r'_1, T_H)$  and  $(r'_2, T_H)$  with  $r_2 > r_1$  and

$\alpha$	$\mathcal{L}_\alpha(r_0)$
1	$\sqrt{R_n \frac{\kappa m (T_L/m)^{1/n}}{\lambda_0^{f_n} e^{f_n r_0}} (1 - \sqrt{T_L/T_H})}$
$n + 1$	$\sqrt{\frac{T_H}{\kappa} (1 - \sqrt{T_L/T_H})}$

Table I. Expressions of the thermodynamic lengths of the exponential paths with  $\alpha = 1$  and  $\alpha = n + 1$ .

$r'_2 > r'_1$  in the control-parameter space, and connect these points to form a closed path consisting of two isothermal and two connecting paths. In the optimal protocol of the cycle, the control parameters are varied with the same velocity of the thermodynamic length in both the isothermal and the connecting processes. To achieve possibly large output power, we construct the cycle with a large ratio  $\mathcal{A}/\mathcal{L}$ . An efficient choice of the connecting paths is the geodesic paths according to the metric (15). The explicit expressions of the geodesic equations are left in [50]. Initiated from one point on the low-temperature line  $T = T_L$ , we solve the shortest geodesic path to reach the high-temperature line  $T = T_H$  with the shooting method [52] (green solid curves in Fig. 1). We choose the two connecting paths as the shortest geodesic paths. Thus,  $r'_i$  is determined by  $r_i$ . The area  $\mathcal{A}_{\text{geo}}(r_1, r_2)$  and the thermodynamic length  $\mathcal{L}_{\text{geo}}(r_1, r_2)$  of the cycle are functions of  $r_1$  and  $r_2$ , and can be numerically calculated.

We can alternatively choose the connecting paths as the exponential path  $T(r) = T_L \exp[\alpha(r - r_0)]$ ,  $r_0 \leq r \leq r'_0 := r_0 + \ln(T_H/T_L)/\alpha$ . The thermodynamic length  $\mathcal{L}_\alpha(r_0)$  of the exponential path is obtained analytically in [50], and given in Table I for  $\alpha = 1$  and  $n + 1$ . For given  $r_0$ , we can also optimize  $\alpha$  to minimize the thermodynamic length  $\mathcal{L}_\alpha(r_0)$  of the exponential path, and obtain the shortest exponential path (orange dotted curve in Fig. 1), which almost coincides with the shortest geodesic path (but not exactly). We remark that the cycles with the exponential paths contain several cycles in classical thermodynamics, e.g., the Carnot ( $\alpha_{1,2} = 1$ ) and the Stirling cycles ( $\alpha_{1,2} = \infty$ ). The quasistatic output work  $-W_o = (f_n/2) \mathcal{A}_{\text{exp}}(r_1, \alpha_1, r_2, \alpha_2)$ , the quasistatic efficiency  $\eta_o$ , and the thermodynamic length  $\mathcal{L}_{\text{exp}}(r_1, \alpha_1, r_2, \alpha_2)$  of these cycles are derived analytically in [50]. We compare the shortest geodesic paths and the shortest exponential paths for the harmonic potential  $n = 1$  in Fig. 1.

Figure 2 shows the control scheme of the heat engine with the shortcut strategy to achieve the maximum power with the boundary values  $r_1 = -1$  and  $r_2 = 0$  of the work parameter. The connecting paths are chosen as the shortest geodesic paths (II and IV). The area and the thermodynamic length of the cycle are  $\mathcal{A}_{\text{geo}}(-1, 0) = 0.546$  and  $\mathcal{L}_{\text{geo}}(-1, 0) = 3.59$ . The maximum power  $P_{\max} = 0.00578$  is reached with the operation time  $\tau_{\max} = 47.2$ . The cycle contains four processes,

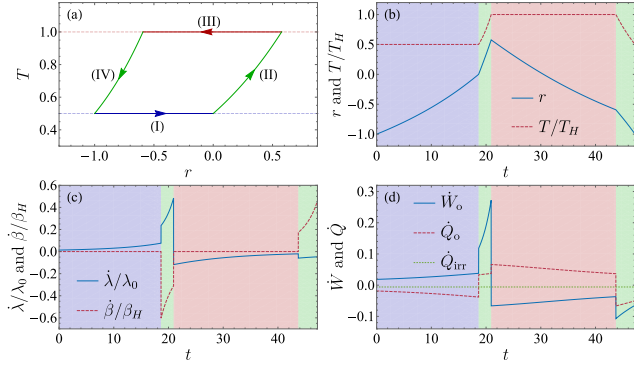


Figure 2. The control scheme to achieve the maximum power. (a) The  $r - T$  diagram with  $r_1 = -1$  and  $r_2 = 0$ . The connecting paths (II and IV) are the shortest geodesic paths. The whole cycle is divided into four processes (I)–(IV). (b) The variation of the control parameters  $r(t)$  and  $T(t)$  in a cycle. (c) The implementation of the auxiliary Hamiltonian represented by  $\dot{\lambda}$  and  $\dot{\beta}$ . (d) The input power  $\dot{W}$  and the heat flux  $\dot{Q}$ .

(I) isothermal compression, (II) connecting compression, (III) isothermal expansion, and (IV) connecting expansion. The control scheme to vary the control parameters  $r(t)$  and  $T(t)$  is shown in Fig. 2(b). Figure 2(c) shows the implementation of the auxiliary Hamiltonian characterized by  $\dot{\lambda}$  and  $\dot{\beta}$ . Figure 2(d) plots the input power and the heat flux in a cycle. The quasistatic heat is absorbed  $\dot{Q}_o > 0$  in processes (II) and (III), and released  $\dot{Q}_o < 0$  in processes (I) and (IV). The irreversible heat flux (9) is  $\dot{Q}_{\text{irr}} = -0.00578$  during the whole cycle.

*Discussions.* In the highly underdamped regime  $\chi \ll 1$ , the thermodynamic length [Eq. (15)] is simplified into  $\mathcal{L}^{\text{under}} = (f_n/2) \oint \sqrt{(T - dT/dr)^2 / (\kappa T)} dr$ , which becomes zero on the exponential paths with  $\alpha = 1$ . The connecting processes on these paths are free of the irreversible work and does not cost any time (compared to the isothermal processes). Thus, we choose two of these exponential paths  $T(r) = T_L \exp(r - r_i)$ ,  $i = 1, 2$  to construct the optimal cycle in the highly underdamped regime. The area of the closed path is

$$\mathcal{A} = (T_H - T_L)(r_2 - r_1). \quad (18)$$

The thermodynamic length of the cycle is [50]

$$\mathcal{L}^{\text{under}} = \frac{f_n}{2} \left( \frac{\sqrt{T_H} + \sqrt{T_L}}{\sqrt{\kappa}} \right) (r_2 - r_1). \quad (19)$$

The maximum power (17) is

$$P_{\text{max}}^{\text{under}} = \frac{\kappa}{4} (\sqrt{T_H} - \sqrt{T_L})^2. \quad (20)$$

The quasistatic cycle is the Carnot cycle with the efficiency  $\eta_o = \eta_C$ . The EMP (11) becomes the Curzon-

Ahlborn efficiency [53]

$$\eta_{\text{EMP}}^{\text{under}} = \eta_{\text{CA}} := 1 - \sqrt{T_L/T_H}, \quad (21)$$

since the highly underdamped regime satisfies the preconditions of the Curzon-Ahlborn heat engines [22]. Both the maximum power (20) and the EMP (21) agree with the results in Refs. [21, 22], and are independent of the shape of the potential  $n$  and the choices of  $r_1$  and  $r_2$ . With the shortcut strategy, the optimal protocol of the cycle and the maximum power at given efficiency differ from those in Refs. [21, 22, 54] (see [50] for the discussion).

In the overdamped regime  $\chi \gg 1$ , the thermodynamic length [Eq. (15)] is simplified into

$$\mathcal{L}^{\text{over}} = \frac{f_n}{2} \oint \sqrt{\frac{\chi}{\kappa T} \left( T dr - \frac{1}{n+1} \frac{dT}{dr} \right)^2} dr, \quad (22)$$

which becomes zero on the exponential paths with  $\alpha = n + 1$ . The optimal cycle in the overdamped regime are constructed with two of these exponential paths  $T(r) = T_L \exp[(n+1)(r - r_i)]$ ,  $i = 1, 2$ . The area of the closed path is also given by Eq. (18), while the thermodynamic length of the cycle is

$$\mathcal{L}^{\text{over}} = 2 \sqrt{R_n \frac{\kappa m}{\lambda_0} \left( \frac{T_L}{\lambda_0 m} \right)^{1/n} \left( e^{-f_n r_1/2} - e^{-f_n r_2/2} \right)}. \quad (23)$$

The maximum power (17) is

$$P_{\text{max}}^{\text{over}} = \frac{f_n^2}{64 R_n} \frac{\lambda_0^{f_n} m^{1/n}}{\kappa m T_L^{1/n}} \frac{(T_H - T_L)^2 (r_2 - r_1)^2}{(e^{-f_n r_1/2} - e^{-f_n r_2/2})^2}. \quad (24)$$

The efficiency of the quasistatic cycle is [50]

$$\eta_o^{\text{over}} = \frac{\eta_C}{1 + \eta_C / \{f_n (r_2 - r_1)\}}, \quad (25)$$

which deviates from the Carnot efficiency due to extra heat exchange from the kinetic energy change. The EMP (11) is

$$\eta_{\text{EMP}}^{\text{over}} = \frac{\eta_C}{2 + \{4/[f_n (r_2 - r_1)] - 1\} \eta_C / 2}. \quad (26)$$

Both the maximum power (24) and the EMP (26) agree with the results in Ref. [24]. The optimal protocol with the shortcut strategy in the overdamped regime also converges to the control scheme of Ref. [24] since the auxiliary Hamiltonian becomes a potential of the position in the overdamped regime (see [50] for the discussion).

Figure 3 shows the maximum power  $P_{\text{max}}$  and the EMP  $\eta_{\text{EMP}}$  of different cycles in the general-damped situation. We choose the connecting paths as the shortest

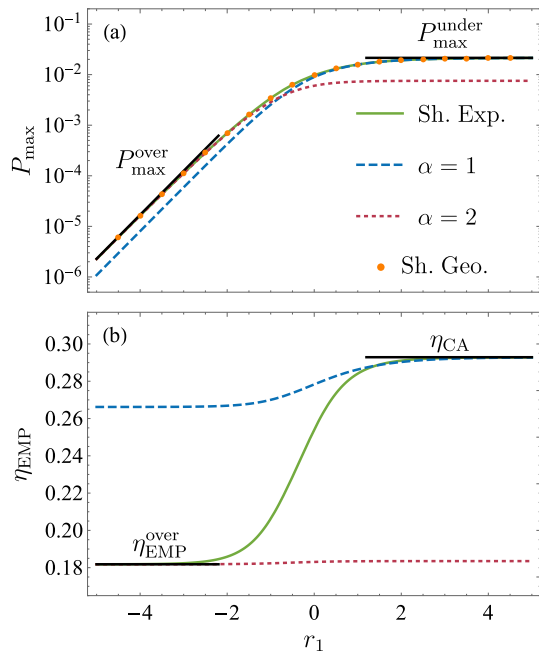


Figure 3. The maximum power and the EMP as functions of  $r_1$ . We set  $r_2 = r_1 + 0.5$ , and choose the connecting paths as the shortest exponential paths (green solid curve) and the exponential paths with fixed  $\alpha_{1,2} = 1$  (blue dashed curve) and  $\alpha_{1,2} = 2$  (red dotted curve). (a) The maximum power  $P_{\max}$ . The orange dots are the results for the shortest geodesic paths. (b) The EMP  $\eta_{\text{EMP}}$  of the cycle.

exponential paths or the exponential paths with fixed  $\alpha_{1,2} = 1$  and  $\alpha_{1,2} = 2$ . In Fig. 3(a), almost the same maximum power is reached for the shortest exponential paths and the shortest geodesic paths (orange dots). The black solid lines represent the bounds (20) and (24) of the output power obtained in the highly underdamped and the overdamped regimes. In Fig. 3(b), the EMP  $\eta_{\text{EMP}}$  of the cycles with the shortest exponential paths approaches the Curzon-Ahlborn efficiency (21) in the highly underdamped regime and Eq. (26) in the overdamped regime.

*Conclusion.* Based on the shortcut strategy [25, 26, 35], we formulate a geometric description of the energetics in shortcut processes with both work parameter and temperature time-dependent. The thermodynamic length not only provides a tight and reachable bound of the irreversible work, but also guides designing the optimal protocol of either a single process or a heat-engine cycle. The optimal protocol is to vary the control parameters with a constant velocity of the thermodynamic length.

We employ the shortcut strategy to design and optimize the Brownian heat engine, and obtain the optimal protocol of the cycle. The maximum power, the EMP, and the maximum power at given efficiency are all related to the thermodynamic length. Such optimization can be further extended to specific cycles, e.g., Carnot, Otto, and Stirling cycles, etc. We illustrate that the EMP

approaches the Curzon-Ahlborn efficiency in the highly underdamped regime [21, 22], and converges to the result [24] in the overdamped regime. We conclude this Letter that the shortcut strategy is a powerful method for optimizing the performance of heat engines, and may also be beneficial for the experimental realization of Brownian heat engines [9].

*Note added:* We notice a related recent work [55], where shortcuts to adiabaticity and shortcuts to isothermality are introduced simultaneously to realize finite-time Carnot cycles.

J.F.C thanks Hui Dong and H.T. Quan for carefully reading the manuscript. This work is supported by the National Natural Science Foundation of China (NSFC) under Grants No. 11775001, No. 11825501, and No. 12147157.

\* chenjinfu@pku.edu.cn

- [1] K. Sekimoto, *Stochastic Energetics* (Springer-Verlag GmbH, 2010).
- [2] C. Jarzynski, Equalities and Inequalities: Irreversibility and the Second Law of Thermodynamics at the Nanoscale, *Annu. Rev. Condens. Matter Phys.* **2**, 329 (2011).
- [3] U. Seifert, Stochastic thermodynamics, fluctuation theorems and molecular machines, *Rep. Prog. Phys.* **75**, 126001 (2012).
- [4] C. V. den Broeck and M. Esposito, Ensemble and trajectory thermodynamics: A brief introduction, *Phys. A (Amsterdam, Neth.)* **418**, 6 (2015).
- [5] M. Esposito, U. Harbola, and S. Mukamel, Nonequilibrium fluctuations, fluctuation theorems, and counting statistics in quantum systems, *Rev. Mod. Phys.* **81**, 1665 (2009).
- [6] M. Campisi, P. Hänggi, and P. Talkner, Colloquium: Quantum fluctuation relations: Foundations and applications, *Rev. Mod. Phys.* **83**, 771 (2011).
- [7] V. Holubec and A. Ryabov, Fluctuations in heat engines, *J. Phys. A: Math. Theor.* **55**, 013001 (2021).
- [8] O. Abah, J. Roßnagel, G. Jacob, S. Deffner, F. Schmidt-Kaler, K. Singer, and E. Lutz, Single-Ion Heat Engine at Maximum Power, *Phys. Rev. Lett.* **109**, 203006 (2012).
- [9] I. A. Martínez, É. Roldán, L. Dinis, D. Petrov, J. M. R. Parrondo, and R. A. Rica, Brownian Carnot engine, *Nat. Phys.* **12**, 67 (2015).
- [10] M. H. Rubin, Optimal configuration of a class of irreversible heat engines. I, *Phys. Rev. A* **19**, 1272 (1979).
- [11] M. H. Rubin, Optimal configuration of a class of irreversible heat engines. II, *Phys. Rev. A* **19**, 1277 (1979).
- [12] V. Cavina, A. Mari, A. Carlini, and V. Giovannetti, Optimal thermodynamic control in open quantum systems, *Phys. Rev. A* **98**, 012139 (2018).
- [13] P. Salamon and R. S. Berry, Thermodynamic Length and Dissipated Availability, *Phys. Rev. Lett.* **51**, 1127 (1983).
- [14] G. E. Crooks, Measuring Thermodynamic Length, *Phys. Rev. Lett.* **99**, 100602 (2007).
- [15] D. A. Sivak and G. E. Crooks, Thermodynamic Metrics and Optimal Paths, *Phys. Rev. Lett.* **108**, 190602 (2012).

- [16] Z. Gong, Y. Lan, and H. T. Quan, Stochastic Thermodynamics of a Particle in a Box, *Phys. Rev. Lett.* **117**, 180603 (2016).
- [17] M. Scandi and M. Perarnau-Llobet, Thermodynamic length in open quantum systems, *Quantum* **3**, 197 (2019).
- [18] K. Brandner and K. Saito, Thermodynamic Geometry of Microscopic Heat Engines, *Phys. Rev. Lett.* **124**, 040602 (2020).
- [19] D. S. P. Salazar, Work distribution in thermal processes, *Phys. Rev. E* **101**, 030101(R) (2020).
- [20] J.-F. Chen, C. P. Sun, and H. Dong, Extrapolating the thermodynamic length with finite-time measurements, *Phys. Rev. E* **104**, 034117 (2021).
- [21] A. Dechant, N. Kiesel, and E. Lutz, Underdamped stochastic heat engine at maximum efficiency, *Europhys. Lett.* **119**, 50003 (2017).
- [22] Y. H. Chen, J.-F. Chen, Z. Fei, and H. T. Quan, A microscopic theory of Curzon-Ahlborn heat engine, (2021), arXiv:2108.04128 [cond-mat.stat-mech].
- [23] T. Schmiedl and U. Seifert, Optimal Finite-Time Processes In Stochastic Thermodynamics, *Phys. Rev. Lett.* **98**, 108301 (2007).
- [24] T. Schmiedl and U. Seifert, Efficiency at maximum power: An analytically solvable model for stochastic heat engines, *Europhys. Lett.* **81**, 20003 (2007).
- [25] I. A. Martínez, A. Petrosyan, D. Guéry-Odelin, E. Trizac, and S. Ciliberto, Engineered swift equilibration of a Brownian particle, *Nat. Phys.* **12**, 843 (2016).
- [26] G. Li, H. T. Quan, and Z. C. Tu, Shortcuts to isothermality and nonequilibrium work relations, *Phys. Rev. E* **96**, 012144 (2017).
- [27] J. A. C. Albay, S. R. Wulaningrum, C. Kwon, P.-Y. Lai, and Y. Jun, Thermodynamic cost of a shortcuts-to-isothermal transport of a Brownian particle, *Phys. Rev. Research* **1**, 033122 (2019).
- [28] J. A. C. Albay, P.-Y. Lai, and Y. Jun, Realization of finite-rate isothermal compression and expansion using optical feedback trap, *Appl. Phys. Lett.* **116**, 103706 (2020).
- [29] J. A. C. Albay, C. Kwon, P.-Y. Lai, and Y. Jun, Work relation in instantaneous-equilibrium transition of forward and reverse processes, *New J. Phys.* **22**, 123049 (2020).
- [30] N. Pancotti, M. Scandi, M. T. Mitchison, and M. Perarnau-Llobet, Speed-Ups to Isothermality: Enhanced Quantum Thermal Machines through Control of the System-Bath Coupling, *Phys. Rev. X* **10**, 031015 (2020).
- [31] K. Nakamura, J. Matrasulov, and Y. Izumida, Fast-forward approach to stochastic heat engine, *Phys. Rev. E* **102**, 012129 (2020).
- [32] C. A. Plata, D. Guéry-Odelin, E. Trizac, and A. Prados, Building an irreversible Carnot-like heat engine with an overdamped harmonic oscillator, *J. Stat. Mech.: Theory Exp.* **2020**, 093207 (2020).
- [33] S. Iram, E. Dolson, J. Chiel, J. Pelesko, N. Krishnan, Özenç Güngör, B. Kuznets-Speck, S. Deffner, E. Ilker, J. G. Scott, and M. Hinczewski, Controlling the speed and trajectory of evolution with counterdiabatic driving, *Nat. Phys.* **17**, 135 (2020).
- [34] E. Ilker, Özenç Güngör, B. Kuznets-Speck, J. Chiel, S. Deffner, and M. Hinczewski, Shortcuts in stochastic systems and control of biophysical processes, (2021), arXiv:2106.07130 [cond-mat.stat-mech].
- [35] Y. Jun and P.-Y. Lai, Instantaneous equilibrium transition for Brownian systems under time-dependent temperature and potential variations: Reversibility, heat and work relations, and fast isentropic process, *Phys. Rev. Research* **3**, 033130 (2021).
- [36] Y. Jun and P.-Y. Lai, Minimal dissipation protocols of an instantaneous equilibrium Brownian particle under time-dependent temperature and potential variations, *Phys. Rev. Research* **4**, 023157 (2022).
- [37] G. Li, J.-F. Chen, C. P. Sun, and H. Dong, Geodesic Path for the Minimal Energy Cost in Shortcuts to Isothermality, *Phys. Rev. Lett.* **128**, 230603 (2022).
- [38] M. Esposito, R. Kawai, K. Lindenberg, and C. V. den Broeck, Efficiency at Maximum Power of Low-Dissipation Carnot Engines, *Phys. Rev. Lett.* **105**, 150603 (2010).
- [39] Z.-C. Tu, Recent advance on the efficiency at maximum power of heat engines, *Chin. Phys. B* **21**, 020513 (2012).
- [40] Y. Wang and Z. C. Tu, Efficiency at maximum power output of linear irreversible Carnot-like heat engines, *Phys. Rev. E* **85**, 011127 (2012).
- [41] A. Ryabov and V. Holubec, Maximum efficiency of steady-state heat engines at arbitrary power, *Phys. Rev. E* **93**, 050101(R) (2016).
- [42] V. Cavina, A. Mari, and V. Giovannetti, Slow Dynamics and Thermodynamics of Open Quantum Systems, *Phys. Rev. Lett.* **119**, 050601 (2017).
- [43] Y.-H. Ma, D. Xu, H. Dong, and C.-P. Sun, Universal constraint for efficiency and power of a low-dissipation heat engine, *Phys. Rev. E* **98**, 042112 (2018).
- [44] P. Abiuso and M. Perarnau-Llobet, Optimal Cycles for Low-Dissipation Heat Engines, *Phys. Rev. Lett.* **124**, 110606 (2020).
- [45] A. G. Frim and M. R. DeWeese, Geometric Bound on the Efficiency of Irreversible Thermodynamic Cycles, *Phys. Rev. Lett.* **128**, 230601 (2022).
- [46] G. Watanabe and Y. Minami, Finite-time thermodynamics of fluctuations in microscopic heat engines, *Phys. Rev. Research* **4**, L012008 (2022).
- [47] H. Yuan, Y.-H. Ma, and C. P. Sun, Optimizing thermodynamic cycles with two finite-sized reservoirs, *Phys. Rev. E* **105**, L022101 (2022).
- [48] Z. Ye, F. Cerisola, P. Abiuso, J. Anders, M. Perarnau-Llobet, and V. Holubec, Optimal finite-time heat engines under constrained control, (2022), arXiv:2202.12953 [cond-mat.stat-mech].
- [49] H. A. Kramers, Brownian motion in a field of force and the diffusion model of chemical reactions, *Physica* **7**, 284 (1940).
- [50] “See supplementary material.”.
- [51] This parameterization simplifies the expressions of the thermodynamic length, and allows the same optimal protocol to vary  $\lambda$  in the highly underdamped regime. For the harmonic potential ( $n = 1$ ), the work parameter  $\lambda$  becomes the frequency.
- [52] M. Berger, *A Panoramic View of Riemannian Geometry* (Springer Berlin Heidelberg, 2007).
- [53] F. L. Curzon and B. Ahlborn, Efficiency of a Carnot engine at maximum power output, *Am. J. Phys.* **43**, 22 (1975).
- [54] L. Chen and Z. Yan, The effect of heat-transfer law on performance of a two-heat-source endoreversible cycle, *J. Chem. Phys.* **90**, 3740 (1989).
- [55] X.-H. Zhao, Z.-N. Gong, and Z. C. Tu, Microscopic low-dissipation heat engine via shortcuts to adiabaticity

and shortcuts to isothermality, (2022), arXiv:2206.02337  
[cond-mat.stat-mech].



# Supplementary material: Optimizing Brownian heat engine with shortcut strategy

Jin-Fu Chen<sup>1,\*</sup>

<sup>1</sup>*School of Physics, Peking University, Beijing, 100871, China*

We show derivations to the results of the main text, and discuss the optimal protocols of the cycles in the highly underdamped regime and the overdamped regime. In Section I, we show the implementation of the auxiliary Hamiltonian in the shortcut strategy, and illustrate work and heat in shortcut processes. Section II gives the explicit results for the power-law potentials. In Section III, we derive the analytical results of the output work, the quasistatic efficiency, and the thermodynamic length for the heat-engine cycles with exponential connecting paths. In Section IV, we derive the maximum power and the efficiency at the maximum power expressed by the thermodynamic length. In Section V, we derive the maximum power at given efficiency. In Sections VI and VII, we show the optimal control schemes of the cycles in the highly underdamped regime and the overdamped regimes. They are compared with the ones obtained in previous works.

## CONTENTS

I. Work and heat in shortcut processes	1
II. Explicit results for the power-law potentials	4
III. Output work, efficiency and thermodynamic length for cycles with exponential connecting paths	6
IV. Maximum power and efficiency at maximum power	9
V. Maximum power at given efficiency	10
VI. Highly underdamped regime $\chi \ll 1$	11
A. Optimal protocol	13
B. Comparison to Refs. [7, 8]	14
VII. Overdamped regime $\chi \gg 1$	15
A. Optimal protocol	17
B. Comparison to Ref. [5]	18
References	19

## I. WORK AND HEAT IN SHORTCUT PROCESSES

We rewrite the Kramer equation [Eq. (1) in the main text] as

$$\frac{\partial \rho}{\partial t} = \mathcal{L}_o[\rho] + \mathcal{D}_o[\rho] + \mathcal{L}_a[\rho] + \mathcal{D}_a[\rho]. \quad (\text{S1})$$

The operators  $\mathcal{L}_o$  and  $\mathcal{D}_o$  reflect the deterministic and the dissipative parts of the evolution subject to the original Hamiltonian  $H_o(x, p, \lambda) = p^2/(2m) + U_o(x, \lambda)$ , and are explicitly

$$\mathcal{L}_o[\rho] = -\frac{\partial}{\partial x} \left( \frac{\partial H_o}{\partial p} \rho \right) + \frac{\partial}{\partial p} \left( \frac{\partial H_o}{\partial x} \rho \right), \quad (\text{S2})$$

$$\mathcal{D}_o[\rho] = \kappa m \frac{\partial}{\partial p} \left( \frac{\partial H_o}{\partial p} \rho + \frac{1}{\beta} \frac{\partial \rho}{\partial p} \right). \quad (\text{S3})$$

The operators  $\mathcal{L}_a$  and  $\mathcal{D}_a$  reflect the deterministic and the dissipative parts of the evolution subject to the auxiliary Hamiltonian  $H_a$ , and are explicitly



$$\mathcal{L}_a[\rho] = -\frac{\partial}{\partial x} \left( \frac{\partial H_a}{\partial p} \rho \right) + \frac{\partial}{\partial p} \left( \frac{\partial H_a}{\partial x} \rho \right), \quad (\text{S4})$$

$$\mathcal{D}_a[\rho] = \kappa m \frac{\partial}{\partial p} \left( \frac{\partial H_a}{\partial p} \rho \right). \quad (\text{S5})$$

The instantaneous equilibrium state  $\rho_{\text{ieq}} := \exp\{\beta[F(\lambda, \beta) - H_o(x, p, \lambda)]\}$  nullifies the operators  $\mathcal{L}_o[\rho_{\text{ieq}}] = 0$  and  $\mathcal{D}_o[\rho_{\text{ieq}}] = 0$ , and its time derivative is

$$\frac{\partial \rho_{\text{ieq}}}{\partial t} = \beta \left[ \frac{\dot{\beta}}{\beta} (F - H_o) + \dot{\beta} \frac{\partial F}{\partial \beta} + \dot{\lambda} \left( \frac{\partial F}{\partial \lambda} - \frac{\partial U_o}{\partial \lambda} \right) \right] \rho_{\text{ieq}}. \quad (\text{S6})$$

Equation (S1) gives the principle to construct the auxiliary Hamiltonian [1]

$$\frac{\partial \rho_{\text{ieq}}}{\partial t} = \mathcal{L}_a[\rho_{\text{ieq}}] + \mathcal{D}_a[\rho_{\text{ieq}}], \quad (\text{S7})$$

which is explicitly

$$\frac{\partial \rho_{\text{ieq}}}{\partial t} = -\frac{\partial H_a}{\partial p} \frac{\partial \rho_{\text{ieq}}}{\partial x} + \frac{\partial H_a}{\partial x} \frac{\partial \rho_{\text{ieq}}}{\partial p} + \kappa m \frac{\partial}{\partial p} \left( \frac{\partial H_a}{\partial p} \rho_{\text{ieq}} \right). \quad (\text{S8})$$

As done in Ref. [2], both the inverse temperature  $\beta(t)$  and the work parameter  $\lambda(t)$  are treated as the time-dependent control parameters. By setting the auxiliary Hamiltonian as

$$H_a = \dot{\lambda} h_\lambda(x, p, \lambda) + \dot{\beta} h_\beta(x, p, \lambda, \beta), \quad (\text{S9})$$

Eqs. (S6) and (S8) lead to the partial differential equations for the auxiliary functions  $h_\lambda(x, p, \lambda)$  and  $h_\beta(x, p, \lambda, \beta)$  as

$$\frac{\kappa m}{\beta} \frac{\partial^2 h_\lambda}{\partial p^2} - \kappa p \frac{\partial h_\lambda}{\partial p} + \frac{\partial U_o}{\partial x} \frac{\partial h_\lambda}{\partial p} - \frac{p}{m} \frac{\partial h_\lambda}{\partial x} = \frac{\partial F}{\partial \lambda} - \frac{\partial U_o}{\partial \lambda}, \quad (\text{S10})$$

$$\frac{\kappa m}{\beta} \frac{\partial^2 h_\beta}{\partial p^2} - \kappa p \frac{\partial h_\beta}{\partial p} + \frac{\partial U_o}{\partial x} \frac{\partial h_\beta}{\partial p} - \frac{p}{m} \frac{\partial h_\beta}{\partial x} = \frac{1}{\beta} (F - H_o) + \frac{\partial F}{\partial \beta}. \quad (\text{S11})$$

The quasistatic work, the quasistatic heat, the irreversible work and the irreversible heat are defined as

$$\dot{W}_o = \dot{\lambda} \iint \frac{\partial U_o}{\partial \lambda} \rho_{\text{ieq}} dx dp, \quad (\text{S12})$$

$$\dot{Q}_o = \iint H_o \frac{\partial \rho_{\text{ieq}}}{\partial t} dx dp, \quad (\text{S13})$$

$$\dot{W}_{\text{irr}} = \iint \frac{\partial H_a}{\partial t} \rho_{\text{ieq}} dx dp, \quad (\text{S14})$$

$$\dot{Q}_{\text{irr}} = \iint H_a \frac{\partial \rho_{\text{ieq}}}{\partial t} dx dp. \quad (\text{S15})$$

Plugging Eq. (S8) into Eq. (S15), we obtain the irreversible heat as

$$\frac{dQ_{\text{irr}}}{dt} = \iint \left\{ \begin{aligned} & (\dot{\lambda} h_\lambda + \dot{\beta} h_\beta) \dot{\lambda} \left[ \frac{\partial h_\lambda}{\partial x} \frac{\partial \rho_{\text{ieq}}}{\partial p} - \frac{\partial h_\lambda}{\partial p} \frac{\partial \rho_{\text{ieq}}}{\partial x} + \kappa m \frac{\partial}{\partial p} \left( \frac{\partial h_\lambda}{\partial p} \rho_{\text{ieq}} \right) \right] \\ & + (\dot{\lambda} h_\lambda + \dot{\beta} h_\beta) \dot{\beta} \left[ \frac{\partial h_\beta}{\partial x} \frac{\partial \rho_{\text{ieq}}}{\partial p} - \frac{\partial h_\beta}{\partial p} \frac{\partial \rho_{\text{ieq}}}{\partial x} + \kappa m \frac{\partial}{\partial p} \left( \frac{\partial h_\beta}{\partial p} \rho_{\text{ieq}} \right) \right] \end{aligned} \right\} dx dp. \quad (\text{S16})$$

We show the calculation for each term

$$\iint (\dot{\lambda}h_\lambda + \dot{\beta}h_\beta) \dot{\lambda} \left[ \frac{\partial h_\lambda}{\partial x} \frac{\partial \rho_{\text{ieq}}}{\partial p} - \frac{\partial h_\lambda}{\partial p} \frac{\partial \rho_{\text{ieq}}}{\partial x} \right] dx dp \quad (\text{S17})$$

$$= \iint -\dot{\lambda} \frac{\partial}{\partial p} \left[ (\dot{\lambda}h_\lambda + \dot{\beta}h_\beta) \frac{\partial h_\lambda}{\partial x} \right] \rho_{\text{ieq}} + \dot{\lambda} \frac{\partial}{\partial x} \left[ (\dot{\lambda}h_\lambda + \dot{\beta}h_\beta) \frac{\partial h_\lambda}{\partial p} \right] \rho_{\text{ieq}} dx dp \quad (\text{S18})$$

$$= \dot{\lambda} \dot{\beta} \iint \left( \frac{\partial h_\beta}{\partial x} \frac{\partial h_\lambda}{\partial p} - \frac{\partial h_\beta}{\partial p} \frac{\partial h_\lambda}{\partial x} \right) \rho_{\text{ieq}} dx dp \quad (\text{S19})$$

$$= \dot{\lambda} \dot{\beta} \left[ \left\langle \frac{\partial h_\lambda}{\partial p} \frac{\partial h_\beta}{\partial x} \right\rangle - \left\langle \frac{\partial h_\lambda}{\partial x} \frac{\partial h_\beta}{\partial p} \right\rangle \right], \quad (\text{S20})$$

where we do the partial integral in the second line, and the boundary term vanishes for the trapped potential. In the last line, the average  $\langle \cdot \rangle$  is over the instantaneous equilibrium state  $\rho_{\text{ieq}}$ . We next calculate

$$\iint (\dot{\lambda}h_\lambda + \dot{\beta}h_\beta) \dot{\lambda} \kappa m \frac{\partial}{\partial p} \left( \frac{\partial h_\lambda}{\partial p} \rho_{\text{ieq}} \right) dx dp \quad (\text{S21})$$

$$= \iint - \left( \dot{\lambda} \frac{\partial h_\lambda}{\partial p} + \dot{\beta} \frac{\partial h_\beta}{\partial p} \right) \dot{\lambda} \kappa m \frac{\partial h_\lambda}{\partial p} \rho_{\text{ieq}} dx dp \quad (\text{S22})$$

$$= -\dot{\lambda} \kappa m \left( \dot{\lambda} \left\langle \frac{\partial h_\lambda}{\partial p} \frac{\partial h_\lambda}{\partial p} \right\rangle + \dot{\beta} \left\langle \frac{\partial h_\lambda}{\partial p} \frac{\partial h_\beta}{\partial p} \right\rangle \right). \quad (\text{S23})$$

It is similar to obtain

$$\iint (\dot{\lambda}h_\lambda + \dot{\beta}h_\beta) \dot{\beta} \left[ \frac{\partial h_\beta}{\partial x} \frac{\partial \rho_{\text{ieq}}}{\partial p} - \frac{\partial h_\beta}{\partial p} \frac{\partial \rho_{\text{ieq}}}{\partial x} \right] dx dp = \dot{\lambda} \dot{\beta} \left( \left\langle \frac{\partial h_\lambda}{\partial x} \frac{\partial h_\beta}{\partial p} \right\rangle - \left\langle \frac{\partial h_\lambda}{\partial p} \frac{\partial h_\beta}{\partial x} \right\rangle \right), \quad (\text{S24})$$

which cancels out the first term [Eq. (S17)]. The last term is

$$\iint (\dot{\lambda}h_\lambda + \dot{\beta}h_\beta) \kappa m \frac{\partial}{\partial p} \left( \frac{\partial h_\beta}{\partial p} \rho_{\text{ieq}} \right) dx dp = -\kappa m \left( \dot{\lambda} \left\langle \frac{\partial h_\lambda}{\partial p} \frac{\partial h_\beta}{\partial p} \right\rangle + \dot{\beta} \left\langle \frac{\partial h_\beta}{\partial p} \frac{\partial h_\beta}{\partial p} \right\rangle \right). \quad (\text{S25})$$

Collecting all the terms, we obtain the explicit expression of the irreversible heat as

$$\frac{dQ_{\text{irr}}}{dt} = - \begin{pmatrix} \dot{\lambda} & \dot{\beta} \end{pmatrix} \mathbf{g} \begin{pmatrix} \dot{\lambda} \\ \dot{\beta} \end{pmatrix}, \quad (\text{S26})$$

with the metric

$$\mathbf{g} = \kappa m \begin{pmatrix} \left\langle \frac{\partial h_\lambda}{\partial p} \frac{\partial h_\lambda}{\partial p} \right\rangle & \left\langle \frac{\partial h_\lambda}{\partial p} \frac{\partial h_\beta}{\partial p} \right\rangle \\ \left\langle \frac{\partial h_\lambda}{\partial p} \frac{\partial h_\beta}{\partial p} \right\rangle & \left\langle \frac{\partial h_\beta}{\partial p} \frac{\partial h_\beta}{\partial p} \right\rangle \end{pmatrix}. \quad (\text{S27})$$

The metric  $\mathbf{g}$  is positive semi-definite since

$$\begin{pmatrix} \dot{\lambda} & \dot{\beta} \end{pmatrix} \mathbf{g} \begin{pmatrix} \dot{\lambda} \\ \dot{\beta} \end{pmatrix} = \kappa m \left\langle \left( \dot{\lambda} \frac{\partial h_\lambda}{\partial p} + \dot{\beta} \frac{\partial h_\beta}{\partial p} \right)^2 \right\rangle \quad (\text{S28})$$

$$= \kappa m \iint \left( \dot{\lambda} \frac{\partial h_\lambda}{\partial p} + \dot{\beta} \frac{\partial h_\beta}{\partial p} \right)^2 \rho_{\text{ieq}} dx dp \geq 0. \quad (\text{S29})$$

The irreversible work is

$$\frac{dW_{\text{irr}}}{dt} = \frac{d\langle H_a \rangle}{dt} + \begin{pmatrix} \dot{\lambda} & \dot{\beta} \end{pmatrix} \mathbf{g} \begin{pmatrix} \dot{\lambda} \\ \dot{\beta} \end{pmatrix}. \quad (\text{S30})$$

Notice that the total differential term  $d\langle H_a \rangle / dt$  does not contribute to the irreversible work. The auxiliary Hamiltonian is switched on at the beginning and off at the end of the process, or changes cyclically in a heat-engine cycle. By using the Cauchy-Schwarz inequality, the integral of the second term is bounded by

$$\int_0^\tau (\dot{\lambda} \ \dot{\beta}) \mathbf{g} \left( \begin{matrix} \dot{\lambda} \\ \dot{\beta} \end{matrix} \right) dt \cdot \tau \geq \left( \int_0^\tau \sqrt{(\dot{\lambda} \ \dot{\beta}) \mathbf{g} \left( \begin{matrix} \dot{\lambda} \\ \dot{\beta} \end{matrix} \right)} dt \right)^2 = \mathcal{L}^2, \quad (\text{S31})$$

where the thermodynamic length is defined as

$$\mathcal{L} := \int_0^1 \sqrt{(\lambda'(s) \ \beta'(s)) \mathbf{g} \left( \begin{matrix} \lambda'(s) \\ \beta'(s) \end{matrix} \right)} ds. \quad (\text{S32})$$

The path in the control-parameter space is parameterized by  $(\lambda(s), \beta(s))$  with  $s \in [0, 1]$ . The integral in Eq. (S32) is independent of the protocol and the operation time. The bound (1) of the irreversible work in the main text follows immediately from the inequality (S31).

## II. EXPLICIT RESULTS FOR THE POWER-LAW POTENTIALS

For the power-law potential  $U_o(x, \lambda) = m\lambda^{n+1}x^{2n}/(2n)$ , the partition function is

$$Z_\lambda(\beta) := \iint e^{-\beta H_o} dx dp = 2^{\frac{1}{2n} + \frac{3}{2}} \sqrt{\frac{m\pi}{\beta}} \lambda^{-\frac{n+1}{2n}} \Gamma\left(1 + \frac{1}{2n}\right) \left(\frac{\beta m}{n}\right)^{-\frac{1}{2n}}, \quad (\text{S33})$$

with the gamma function  $\Gamma(x) = \int_0^{+\infty} t^{x-1} e^{-t} dt$ . The moments of the momentum and position are obtained as

$$\langle p^2 \rangle = \frac{m}{\beta}, \quad (\text{S34})$$

$$\langle x^2 \rangle = \frac{R_n}{\lambda} \frac{1}{(\beta\lambda m)^{1/n}}, \quad (\text{S35})$$

$$\langle x^{2n} \rangle = \frac{1}{\beta m \lambda^{n+1}}, \quad (\text{S36})$$

where  $R_n$  is a pure number

$$R_n = (2n)^{\frac{1}{n}} \frac{\Gamma\left(\frac{3}{2n}\right)}{\Gamma\left(\frac{1}{2n}\right)}. \quad (\text{S37})$$

The auxiliary functions  $h_\lambda(x, p, \lambda)$  and  $h_\beta(x, p, \lambda, \beta)$  are given in the main text, and the average values of them are

$$\langle h_\lambda \rangle = \frac{(n+1)^2}{4\kappa n^2 \lambda \beta} + \frac{n+1}{4\lambda^2 n} \frac{R_n \kappa m}{(\beta\lambda m)^{1/n}}, \quad (\text{S38})$$

$$\langle h_\beta \rangle = \frac{(n+1)^2}{4n^2} \frac{1}{\kappa \beta^2} + \frac{\kappa m}{4n\lambda \beta} \frac{R_n}{(\beta\lambda m)^{1/n}}. \quad (\text{S39})$$

The average values of the original Hamiltonian and the auxiliary Hamiltonian are

$$\langle H_o \rangle = \frac{n+1}{2n\beta}, \quad (\text{S40})$$

$$\langle H_a \rangle = \frac{(n+1)^2}{4\kappa n^2 \beta} \left( \frac{\dot{\lambda}}{\lambda} + \frac{\dot{\beta}}{\beta} \right) + \frac{\kappa m}{4n\lambda} \frac{R_n}{(\beta\lambda m)^{1/n}} \left[ (n+1) \frac{\dot{\lambda}}{\lambda} + \frac{\dot{\beta}}{\beta} \right]. \quad (\text{S41})$$

The explicit results of the quasistatic work, the quasistatic heat, the irreversible work and the irreversible heat are

$$\frac{dW_o}{dt} = \frac{n+1}{2n\beta} \frac{\dot{\lambda}}{\lambda}, \quad (\text{S42})$$

$$\frac{dQ_o}{dt} = -\frac{n+1}{2n\beta} \left( \frac{\dot{\lambda}}{\lambda} + \frac{\dot{\beta}}{\beta} \right), \quad (\text{S43})$$

$$\frac{dW_{\text{irr}}}{dt} = \frac{d\langle H_a \rangle}{dt} + \frac{(n+1)^2}{4n^2} \left[ \frac{1}{\kappa\beta} \left( \frac{\dot{\lambda}}{\lambda} + \frac{\dot{\beta}}{\beta} \right)^2 + \frac{\kappa m}{\lambda} \frac{R_n}{(\lambda m \beta)^{1/n}} \left( \frac{\dot{\lambda}}{\lambda} + \frac{\dot{\beta}}{(n+1)\beta} \right)^2 \right], \quad (\text{S44})$$

$$\frac{dQ_{\text{irr}}}{dt} = -\frac{(n+1)^2}{4n^2} \left[ \frac{1}{\kappa\beta} \left( \frac{\dot{\lambda}}{\lambda} + \frac{\dot{\beta}}{\beta} \right)^2 + \frac{\kappa m}{\lambda} \frac{R_n}{(\lambda m \beta)^{1/n}} \left( \frac{\dot{\lambda}}{\lambda} + \frac{\dot{\beta}}{(n+1)\beta} \right)^2 \right]. \quad (\text{S45})$$

For a heat-engine cycle, the irreversible work of a cycle is

$$W_{\text{irr}} = \frac{(n+1)^2}{4n^2} \int_0^\tau \left[ \frac{1}{\kappa\beta} \left( \frac{\dot{\lambda}}{\lambda} + \frac{\dot{\beta}}{\beta} \right)^2 + \frac{\kappa m}{\lambda} \frac{R_n}{(\lambda m \beta)^{1/n}} \left( \frac{\dot{\lambda}}{\lambda} + \frac{\dot{\beta}}{(n+1)\beta} \right)^2 \right] dt, \quad (\text{S46})$$

and the thermodynamic length is

$$\mathcal{L} = \frac{n+1}{2n} \oint \left\{ \frac{1}{\kappa\beta} \left[ \frac{\lambda'(s)}{\lambda} + \frac{\beta'(s)}{\beta} \right]^2 + \frac{\kappa m}{\lambda} \frac{R_n}{(\lambda m \beta)^{1/n}} \left[ \frac{\lambda'(s)}{\lambda} + \frac{\beta'(s)}{(n+1)\beta} \right]^2 \right\}^{\frac{1}{2}} ds, \quad (\text{S47})$$

where  $\lambda(s)$  and  $\beta(s)$  give the path of the cycle in the control parameter space, and the primes denote their derivatives in respect to arc-length parameter  $s$ . Let us define a dimensionless quantity

$$\chi := R_n \frac{\kappa^2 (m\beta)^{1-1/n}}{\lambda^{1+1/n}}. \quad (\text{S48})$$

The thermodynamic length can be rewritten as

$$\mathcal{L} = \frac{n+1}{2n} \oint \frac{1}{\sqrt{\kappa\beta}} \left\{ \left[ \frac{\lambda'(s)}{\lambda} + \frac{\beta'(s)}{\beta} \right]^2 + \chi \left[ \frac{\lambda'(s)}{\lambda} + \frac{\beta'(s)}{(n+1)\beta} \right]^2 \right\}^{\frac{1}{2}} ds, \quad (\text{S49})$$

The highly underdamped regime is reached when  $\chi \ll 1$ , and the first term dominates in Eq. (S49). The overdamped regime is reached when  $\chi \gg 1$ , and the second term dominates in Eq. (S49).

Equation (15) of the main text is obtained by representing  $\lambda = \lambda_0 e^r$ ,  $\beta = 1/T$  with the new parameters  $r$  and  $T$ . The elements of the metric (S27) expressed by  $r$  and  $T$  are

$$g_{rr} = \frac{(n+1)^2}{4n^2} \left[ \frac{T}{\kappa} + \frac{\kappa m R_n e^{-r}}{\lambda_0} \left( \frac{T e^{-r}}{\lambda_0 m} \right)^{1/n} \right], \quad (\text{S50})$$

$$g_{rT} = -\frac{(n+1)^2}{4n^2 T} \left[ \frac{T}{\kappa} + \frac{\kappa m R_n e^{-r}}{(n+1)\lambda_0} \left( \frac{T e^{-r}}{\lambda_0 m} \right)^{1/n} \right], \quad (\text{S51})$$

$$g_{TT} = \frac{(n+1)^2}{4n^2 T^2} \left[ \frac{T}{\kappa} + \frac{\kappa m R_n e^{-r}}{(n+1)^2 \lambda_0} \left( \frac{T e^{-r}}{\lambda_0 m} \right)^{1/n} \right]. \quad (\text{S52})$$

The Christoffel symbol is determined by the metric as

$$\Gamma^i_{kl} = \frac{1}{2} g^{in} \left( \frac{\partial g_{nk}}{\partial x^l} + \frac{\partial g_{nl}}{\partial x^k} - \frac{\partial g_{kl}}{\partial x^n} \right), \quad (\text{S53})$$

and the geodesic equation is

$$\ddot{x}^i + \Gamma^i_{kl} \dot{x}^k \dot{x}^l = 0. \quad (\text{S54})$$

Here the coordinates  $x^i$  are the control parameters  $r$  and  $T$ . The geodesic equation is explicitly obtained as

$$\ddot{r} = \frac{(n+1)^2}{2n^2 \kappa^2 m^2 R_n} \left( \frac{\lambda_0 m e^r}{T} \right)^{1+\frac{1}{n}} (\dot{T} - T\dot{r})^2 + \frac{(n+1)(n+2)}{2n^2} \dot{r}^2 - \frac{(n+2)}{n^2} \dot{r} \frac{\dot{T}}{T} - \frac{(n-2)}{2n^2} \frac{\dot{T}^2}{T^2}, \quad (\text{S55})$$

$$\frac{\ddot{T}}{T} = \frac{(n+1)^2}{2n^2 \kappa^2 m^2 R_n} \left( \frac{\lambda_0 m e^r}{T} \right)^{1+\frac{1}{n}} (\dot{T} - T\dot{r})^2 + \frac{(n+1)^2}{n^2} \dot{r}^2 - \frac{2(n+1)}{n^2} \dot{r} \frac{\dot{T}}{T} + \frac{(n^2+2)}{2n^2} \frac{\dot{T}^2}{T^2}. \quad (\text{S56})$$

By solving the geodesic equation with the boundary conditions  $(r_i, T_i)$  and  $(r_f, T_f)$ , we obtain the optimal protocol to minimize the irreversible work by varying the control parameters with a constant velocity of the thermodynamic length on the geodesic path. It is difficult to solve the boundary-value problem of the above nonlinear ordinary differential equations, but we can convert it into an initial-value problem. Such a method is known as the shooting method [3]. By solving the geodesic equation with different directions of the initial velocity, we find the shortest geodesic path connecting the point  $(r_0, T_L)$  with the high-temperature isothermal line  $T = T_H$ .

### III. OUTPUT WORK, EFFICIENCY AND THERMODYNAMIC LENGTH FOR CYCLES WITH EXPONENTIAL CONNECTING PATHS

For a realistic heat engine, the control parameters  $r$  and  $T$  are varied under constraints. We consider the temperature  $T$  can be arbitrarily tuned within the range  $T_L \leq T \leq T_H$ . A typical heat-engine cycle with the shortcut strategy is constructed by two isothermal processes (processes I and III) and two connecting processes (processes II and IV).

- Process I: the temperature is  $T = T_L$  with the work parameter varied from  $r_1$  to  $r_2$  ( $r_2 > r_1$ ).
- Process II: the control parameters are varied from  $(r_2, T_L)$  to  $(r'_2, T_H)$ .
- Process III: the temperature is  $T = T_H$  with the work parameter varied from  $r'_2$  to  $r'_1$  ( $r'_2 > r'_1$ ).
- Process IV: the control parameters are varied from  $(r'_1, T_H)$  to  $(r_1, T_L)$ .

We choose the connecting processes with the exponential paths  $T(r) = T_L \exp[\alpha_1(r - r_1)]$ ,  $r_1 \leq r \leq r'_1 := r_1 + \ln(T_H/T_L)/\alpha_1$  (process IV) and  $T(r) = T_L \exp[\alpha_2(r - r_2)]$ ,  $r_2 \leq r \leq r'_2 := r_2 + \ln(T_H/T_L)/\alpha_2$  (process II), and calculate the analytical results of the work and heat. The quasistatic work of the whole cycle is

$$W_o = -\frac{n+1}{2n} \mathcal{A}_{\text{exp}}(r_1, \alpha_1, r_2, \alpha_2) < 0, \quad (\text{S57})$$

which is proportional to the area of the closed path

$$\mathcal{A}_{\text{exp}}(r_1, \alpha_1, r_2, \alpha_2) = (r_2 - r_1)(T_H - T_L) + \left( \frac{1}{\alpha_1} - \frac{1}{\alpha_2} \right) [T_H - T_L - T_H \ln(T_H/T_L)]. \quad (\text{S58})$$

In a quasistatic cycle, the heat is absorbed in process III, and can also be absorbed in processes II and IV according to the values of  $\alpha_2$  and  $\alpha_1$ . The quasistatic heat of the whole cycle is

$$Q_{o,+} = \frac{n+1}{2n} \left\{ (r_2 - r_1) T_H - \left( \frac{1}{\alpha_1} - \frac{1}{\alpha_2} \right) T_H \ln \left( \frac{T_H}{T_L} \right) + \max\left[ \frac{\alpha_2 - 1}{\alpha_2} (T_H - T_L), 0 \right] + \max\left[ -\frac{\alpha_1 - 1}{\alpha_1} (T_H - T_L), 0 \right] \right\}. \quad (\text{S59})$$

The quasistatic efficiency is defined as

$$\eta_o := -\frac{W_o}{Q_{o,+}}, \quad (\text{S60})$$

which is explicitly

$$\eta_o = \frac{(r_2 - r_1)(T_H - T_L) + \left(\frac{1}{\alpha_1} - \frac{1}{\alpha_2}\right)[T_H - T_L - T_H \ln(T_H/T_L)]}{(r_2 - r_1)(T_H) - \left(\frac{1}{\alpha_1} - \frac{1}{\alpha_2}\right)T_H \ln(T_H/T_L) + \max\left[\frac{\alpha_2 - 1}{\alpha_2}(T_H - T_L), 0\right] + \max\left[-\frac{\alpha_1 - 1}{\alpha_1}(T_H - T_L), 0\right]}. \quad (\text{S61})$$

By setting  $\alpha_1 = \alpha_2 = 1$ , the quasistatic cycle is the Carnot cycle, and the quasistatic efficiency becomes the Carnot efficiency  $\eta_o = \eta_C := 1 - T_L/T_H$ .

We next calculate the thermodynamic length. The thermodynamic lengths of the isothermal processes are

$$\mathcal{L}_I = \frac{n+1}{2n} \int_{r_1}^{r_2} \sqrt{\frac{T_L}{\kappa} + R_n \frac{\kappa m}{\lambda_0} e^{-r} \left(\frac{T_L e^{-r}}{\lambda_0 m}\right)^{1/n}} dr \quad (\text{S62})$$

$$= \sqrt{\frac{T_L}{\kappa}} \left[ \sinh^{-1} \left( \sqrt{\frac{\lambda_0 T_L e^r}{\kappa^2 m R_n} \left(\frac{\lambda_0 m e^r}{T_L}\right)^{1/n}} \right) - \sqrt{1 + \frac{\kappa^2 m R_n}{\lambda_0 T_L e^r} \left(\frac{T_L}{\lambda_0 m e^r}\right)^{1/n}} \right] \Bigg|_{r=r_1}^{r_2} \quad (\text{S63})$$

and

$$\mathcal{L}_{III} = \frac{n+1}{2n} \int_{r'_1}^{r'_2} \sqrt{\frac{T_H}{\kappa} + R_n \frac{\kappa m}{\lambda_0} e^{-r} \left(\frac{T_H e^{-r}}{\lambda_0 m}\right)^{1/n}} dr \quad (\text{S64})$$

$$= \sqrt{\frac{T_H}{\kappa}} \left[ \sinh^{-1} \left( \sqrt{\frac{\lambda_0 T_H e^r}{\kappa^2 m R_n} \left(\frac{\lambda_0 m e^r}{T_H}\right)^{1/n}} \right) - \sqrt{1 + \frac{\kappa^2 m R_n}{\lambda_0 T_H e^r} \left(\frac{T_H}{\lambda_0 m e^r}\right)^{1/n}} \right] \Bigg|_{r=r'_1}^{r'_2}. \quad (\text{S65})$$

The thermodynamic length of process II is

$$\mathcal{L}_{II} = \mathcal{L}_{\alpha_2}(r_2) \quad (\text{S66})$$

$$= \frac{n+1}{2n} \int_{r_2}^{r'_2} \sqrt{(1 - \alpha_2)^2 \frac{T_L}{\kappa} e^{\alpha_2(r-r_2)} + \left(1 - \frac{\alpha_2}{n+1}\right)^2 R_n \frac{\kappa m}{\lambda_0} e^{-r} \left(\frac{T_L}{\lambda_0 m} e^{-r+\alpha_2 r - \alpha_2 r_2}\right)^{1/n}} dr \quad (\text{S67})$$

$$= \frac{n+1}{n} \sqrt{\left(\frac{1}{\alpha_2} - \frac{1}{n+1}\right)^2 R_n \frac{\kappa m}{\lambda_0} e^{-r} \left(\frac{T_L}{\lambda_0 m} e^{-r+\alpha_2 r - \alpha_2 r_2}\right)^{1/n}} \left(1 + \Theta_{II} e^{(1+\alpha_2 + \frac{1-\alpha_2}{n})r}\right) \times \left[1 + \frac{1}{2} \Gamma\left(\frac{-1 - \frac{1-\alpha_2}{n}}{2(1+\alpha_2 + \frac{1-\alpha_2}{n})}\right) {}_2\tilde{F}_1\left(1, \frac{\alpha_2}{2(1+\alpha_2 + \frac{1-\alpha_2}{n})}; \frac{1+2\alpha_2 + \frac{1-\alpha_2}{n}}{2(1+\alpha_2 + \frac{1-\alpha_2}{n})}; -\Theta_{II} e^{(1+\alpha_2 + \frac{1-\alpha_2}{n})r}\right)\right] \Bigg|_{r=r_2}^{r'_2}, \quad (\text{S68})$$

where the constant is

$$\Theta_{II} = \frac{(1 - \alpha_2)^2}{\left(1 - \frac{\alpha_2}{n+1}\right)^2} \frac{\lambda_0 T_L e^{-\alpha_2 r_2}}{\kappa^2 m R_n} \left(\frac{\lambda_0 m}{T_L} e^{\alpha_2 r_2}\right)^{1/n}, \quad (\text{S69})$$

and the regularized hyper-geometric function is

$${}_2\tilde{F}_1(a, b; c; z) = \frac{{}_2F_1(a, b; c; z)}{\Gamma(c)} = \frac{1}{\Gamma(c)} \sum_{k=0}^{\infty} \frac{(a)_k (b)_k}{k! (c)_k} z^k, \quad (\text{S70})$$

with the Pochhammer symbol  $(a)_k = \Gamma(a+k)/\Gamma(a)$ . The thermodynamic length of process IV is

$$\mathcal{L}_{\text{IV}} = \mathcal{L}_{\alpha_1}(r_1) \quad (\text{S71})$$

$$= \frac{n+1}{2n} \int_{r_1}^{r_1'} \sqrt{(1-\alpha_1)^2 \frac{T_L}{\kappa} e^{\alpha_1(r-r_1)} + (1-\frac{\alpha_1}{n+1})^2 R_n \frac{\kappa m}{\lambda_0} e^{-r} \left( \frac{T_L}{\lambda_0 m} e^{-r+\alpha_1 r-\alpha_1 r_1} \right)^{1/n}} dr \quad (\text{S72})$$

$$= \frac{n+1}{n} \sqrt{\left( \frac{1}{\alpha_1} - \frac{1}{n+1} \right)^2 R_n \frac{\kappa m}{\lambda_0} e^{-r} \left( \frac{T_L}{\lambda_0 m} e^{-r+\alpha_1 r-\alpha_1 r_1} \right)^{1/n}} \left( 1 + \Theta_{\text{IV}} e^{(1+\alpha_1+\frac{1-\alpha_1}{n})r} \right) \times$$

$$\left[ 1 + \frac{1}{2} \Gamma \left( \frac{-1-\frac{1-\alpha_1}{n}}{2(1+\alpha_1+\frac{1-\alpha_1}{n})} \right) {}_2\tilde{F}_1 \left( 1, \frac{\alpha_1}{2(1+\alpha_1+\frac{1-\alpha_1}{n})}; \frac{1+2\alpha_1+\frac{1-\alpha_1}{n}}{2(1+\alpha_1+\frac{1-\alpha_1}{n})}; -\Theta_{\text{IV}} e^{(1+\alpha_1+\frac{1-\alpha_1}{n})r} \right) \right] \Big|_{r=r_1}^{r_1'}, \quad (\text{S73})$$

where the constant is

$$\Theta_{\text{IV}} = \frac{(1-\alpha_1)^2}{(1-\frac{\alpha_1}{n+1})^2} \frac{\lambda_0 T_L e^{-\alpha_1 r_1}}{\kappa^2 m R_n} \left( \frac{\lambda_0 m}{T_L} e^{\alpha_1 r_1} \right)^{1/n}. \quad (\text{S74})$$

The thermodynamic length of the whole cycle is

$$\mathcal{L}_{\text{exp}}(r_1, \alpha_1, r_2, \alpha_2) = \mathcal{L}_{\text{I}} + \mathcal{L}_{\text{II}} + \mathcal{L}_{\text{III}} + \mathcal{L}_{\text{IV}}. \quad (\text{S75})$$

In the optimal protocol of the cycle, the control parameters are varied with a constant velocity of the thermodynamic length. The operation time consumed in each process is thus proportional to the thermodynamic length of the corresponding path, i.e.,

$$\tau_l = \frac{\mathcal{L}_l}{\mathcal{L}} \tau, \quad (\text{S76})$$

with  $l = \text{I, II, III, and IV}$ . Here,  $\mathcal{L}$  is the thermodynamic length of the closed path, and  $\tau$  is the operation time of the whole cycle.

According to positive and negative sign of the quasistatic heat flux  $\dot{Q}_o > 0$  and  $\dot{Q}_o < 0$ , we divide the whole cycle into the heat absorbed and the heat released paths with the thermodynamic lengths  $\mathcal{L}_+$  and  $\mathcal{L}_-$ , respectively. Here we focus on the optimal protocols on the cycles with exponential connecting paths, and the quasistatic heat flux  $\dot{Q}_o$  does not change sign in each process. In the optimal protocol, the irreversible heat flux  $\dot{Q}_{\text{irr}} = -\mathcal{L}^2/\tau^2$  is a negative constant during the whole cycle. To ensure positive output work, the heat must be absorbed in process III and released in process I. The sign of the quasistatic heat flux  $\dot{Q}_o$  in the two connecting processes II and IV is determined by  $\alpha$  according to Eq. (S59). Then, the thermodynamic length is obtained as

$$\mathcal{L}_+ = \begin{cases} \mathcal{L}_{\text{III}} & \alpha_1 \geq 1, \alpha_2 \leq 1 \\ \mathcal{L}_{\text{III}} + \mathcal{L}_{\text{II}} & \alpha_1 \geq 1, \alpha_2 > 1 \\ \mathcal{L}_{\text{III}} + \mathcal{L}_{\text{IV}} & \alpha_1 < 1, \alpha_2 \leq 1 \\ \mathcal{L}_{\text{III}} + \mathcal{L}_{\text{II}} + \mathcal{L}_{\text{IV}} & \alpha_1 < 1, \alpha_2 > 1 \end{cases}. \quad (\text{S77})$$

We can check the sign by plotting  $\dot{Q}_o$  in a whole cycle [Fig. 2(d) in the main text]. The analytical results obtained in this section are used to plot Fig. 3 of the main text.

We remark that the thermodynamic lengths of the connecting paths are always nonzero in the general damped situation. Thus, the connecting processes consume finite operation time. In the highly underdamped regime  $\chi \ll 1$  and the overdamped regime  $\chi \gg 1$ , we can find specific exponential paths with zero thermodynamic length. The closed path can be constructed using these zero-length paths. In Sections VI and VII, we show explicit results for the highly underdamped regime and the overdamped regime respectively.



#### IV. MAXIMUM POWER AND EFFICIENCY AT MAXIMUM POWER

Since the irreversible work is bounded by  $W_{\text{irr}} \geq \mathcal{L}^2/\tau$ , the output work in a cycle is bounded by

$$-W \leq -W_o - \frac{\mathcal{L}^2}{\tau}. \quad (\text{S78})$$

The output power  $P := -W/\tau$  is bounded by

$$P \leq -\frac{W_o}{\tau} - \frac{\mathcal{L}^2}{\tau^2}, \quad (\text{S79})$$

where the equality is saturated by the optimal protocol of the cycle. By choosing the operation time

$$\tau = \tau_{\text{max}} := \frac{2\mathcal{L}^2}{(-W_o)}, \quad (\text{S80})$$

the maximum power is reached

$$P_{\text{max}} = \frac{(-W_o)^2}{4\mathcal{L}^2}. \quad (\text{S81})$$

The efficiency of the finite-time cycle is defined as

$$\eta := \frac{-W}{Q_+} \quad (\text{S82})$$

$$= -\frac{W_o + W_{\text{irr}}}{Q_{o,+} + Q_{\text{irr},+}}. \quad (\text{S83})$$

In the optimal protocol on a given closed path, the irreversible work is expressed by the thermodynamic length

$$W_{\text{irr}} = \frac{\mathcal{L}^2}{\tau}. \quad (\text{S84})$$

The irreversible heat flux is a negative constant  $\dot{Q}_{\text{irr}} = -\mathcal{L}^2/\tau^2$ , and the irreversible part of the overall heat absorbed is

$$Q_{\text{irr},+} = -\frac{\mathcal{L}}{\tau}\mathcal{L}_+. \quad (\text{S85})$$

Together with the quasistatic efficiency (S60), we obtain the efficiency

$$\eta = \frac{-W_o - \mathcal{L}^2/\tau}{-W_o/\eta_o - \mathcal{L}_+\mathcal{L}/\tau}. \quad (\text{S86})$$

With Eq. (S80), the efficiency at the maximum power is

$$\eta_{\text{EMP}} = \frac{\eta_o}{2 - \eta_o\mathcal{L}_+/\mathcal{L}}. \quad (\text{S87})$$

For the cycles with exponential connecting paths, the maximum power and the efficiency at the maximum power are then obtained with the above analytical results of  $\mathcal{A}_{\text{exp}}$ ,  $\eta_o$ ,  $\mathcal{L}_{\text{exp}}$  and  $\mathcal{L}_+$ .

We presents the results of the maximum power  $P_{\text{max}}$  and the efficiency at the maximum power  $\eta_{\text{EMP}}$  of different cycles with the exponential connecting paths in Fig. S1, where  $P_{\text{max}}$  and  $\eta_{\text{EMP}}$  are functions of  $r_1$  and  $r_2$ . We consider the harmonic potential  $n = 1$ , and the other parameters are chosen as  $\lambda_0 = 1$ ,  $m = 1$ ,  $\kappa = 1$ ,  $T_L = 0.5$ ,

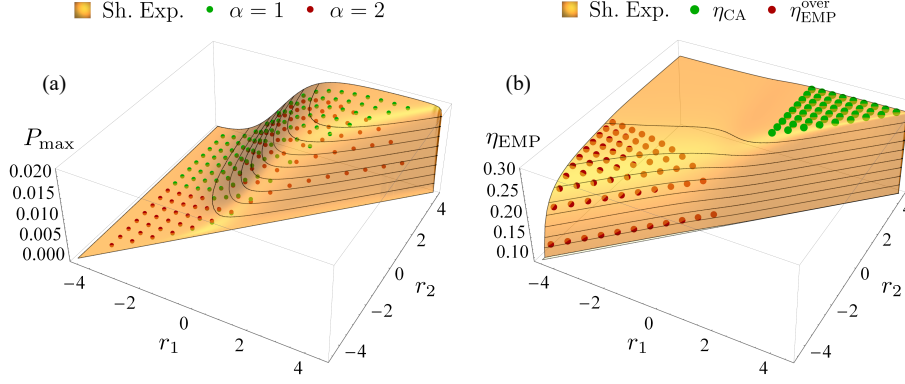


Figure S1. The maximum power and the efficiency at the maximum power as functions of  $r_1$  and  $r_2$ . (a) The maximum power  $P_{\max}$  of the heat-engine cycles with exponential paths, where we choose the shortest exponential paths (orange surface) and the exponential paths with fixed  $\alpha_{1,2} = 1$  (green dots) and  $\alpha_{1,2} = 2$  (red dots). (b) The efficiency at the maximum power  $\eta_{\text{EMP}}$  of the heat-engine cycle with the shortest exponential paths. It approaches the Curzon-Ahlborn efficiency  $\eta_{\text{CA}}$  (green dots) in the highly underdamped regime, and approach  $\eta_{\text{EMP}}^{\text{over}}$  in the overdamped regime (red dots).

and  $T_H = 1$ . Figure S1(a) shows the maximum power  $P_{\max}$  of different heat-engine cycles with exponential paths. The connecting paths are chosen as the shortest exponential paths minimizing  $\mathcal{L}_{\alpha_{1,2}}(r_{1,2})$  (orange surface) and the exponential paths with fixed  $\alpha_{1,2} = 1$  (green dots) and  $\alpha_{1,2} = 2$  (red dots). The maximum power of the cycle with the shortest exponential paths is larger than that of the cycles with fixed  $\alpha_{1,2}$ , and coincides with the results by choosing the connecting paths as the shortest geodesic paths (not shown in the figure). Figure S1(b) shows the efficiency at the maximum power  $\eta_{\text{EMP}}$  for the cycle with the shortest exponential paths. In the highly underdamped regime, the efficiency at the maximum power returns to the Curzon-Ahlborn efficiency [4]  $\eta_{\text{CA}} = 1 - \sqrt{T_L/T_H}$  (green dots). In the overdamped regime, the efficiency at the maximum power agrees with the prediction  $\eta_{\text{EMP}}^{\text{over}} = \eta_o^{\text{over}}/(2 - \eta_o^{\text{over}}/2)$  (red dots) in Ref. [5] where the quasistatic efficiency  $\eta_o^{\text{over}}$  [Eq. (S149)] includes the heat leakage induced by the kinetic energy.

## V. MAXIMUM POWER AT GIVEN EFFICIENCY

From Eq. (S86), we can also calculate the maximum power at given efficiency. By introducing the function

$$\mathcal{F} = \frac{-W_o}{\tau} - \frac{\mathcal{L}^2}{\tau^2} + \zeta \left( \eta - \frac{-W_o - \mathcal{L}^2/\tau}{-W_o/\eta_o - \mathcal{L}_+/\tau} \right), \quad (\text{S88})$$

we calculate the maximum power at given efficiency through

$$\frac{\partial \mathcal{F}}{\partial \tau} = 0, \quad \frac{\partial \mathcal{F}}{\partial \zeta} = 0. \quad (\text{S89})$$

The solution is

$$\tau = \frac{\eta_o(1 - \eta\mathcal{L}_+/\mathcal{L})}{\eta_o - \eta} \frac{\mathcal{L}^2}{(-W_o)}, \quad (\text{S90})$$

and the maximum power at given efficiency is

$$\frac{P_\eta}{P_{\max}} = \frac{4(\eta_o - \eta)(1 - \eta_o\mathcal{L}_+/\mathcal{L})\eta}{\eta_o^2(1 - \eta\mathcal{L}_+/\mathcal{L})^2}. \quad (\text{S91})$$

In the highly underdamped regime, the quasistatic efficiency is the Carnot efficiency  $\eta_o^{\text{under}} = \eta_C$ , and ratio of the thermodynamic lengths is  $\mathcal{L}_+^{\text{under}}/\mathcal{L}^{\text{under}} = \sqrt{T_H}/(\sqrt{T_H} + \sqrt{T_L})$  [see Eq. (S113)]. The maximum power at given efficiency is

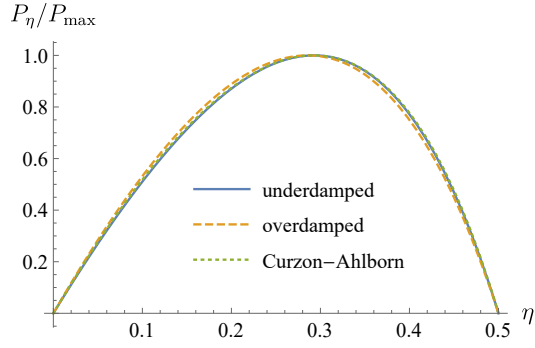


Figure S2. The maximum power at given efficiency. We set  $\eta_C = 1/2$  with  $\eta_{CA} = 1 - 1/\sqrt{2}$  for the highly underdamped regime and  $\eta_o^{\text{over}} = 1/2$  for the overdamped regime.

$$\frac{P_\eta^{\text{under}}}{P_{\text{max}}} = \frac{4\sqrt{T_L/T_H}(\eta_C - \eta)\eta}{(\eta_C - \eta\eta_{CA})^2}. \quad (\text{S92})$$

Notice that the maximum power at given efficiency in the shortcut strategy is different from the one obtained in the highly underdamped regime [6–8]

$$\frac{\tilde{P}_\eta^{\text{under}}}{P_{\text{max}}} = \frac{(\eta_C - \eta)\eta}{(1 - \eta)\eta_{CA}^2}, \quad (\text{S93})$$

but they are quite similar, as shown in Fig. S2. We explain the difference in Section VI.

In the overdamped regime, the quasistatic efficiency  $\eta_o^{\text{over}}$  is given by Eq. (S149), and the ratio of the thermodynamic lengths is  $\mathcal{L}_+^{\text{over}}/\mathcal{L}^{\text{over}} = 1/2$ . The maximum power at given efficiency is

$$\frac{P_\eta^{\text{over}}}{P_{\text{max}}} = \frac{4(\eta_o^{\text{over}} - \eta)(1 - \eta_o^{\text{over}}/2)\eta}{(\eta_o^{\text{over}})^2(1 - \eta_o^{\text{over}}/2)^2}, \quad (\text{S94})$$

where  $\eta_o^{\text{over}}$  is given by Eq. (S149).

In Fig. S2, we show the maximum power at given efficiency in the highly underdamped and the overdamped regimes by setting  $\eta_C = 1/2$  and  $\eta_o^{\text{over}} = 1/2$ . We also show the maximum power at given efficiency [Eq. (S93)] for the Curzon-Ahlborn heat engine [6–8], which is quite similar to that with the shortcut strategy in the highly underdamped regime.

## VI. HIGHLY UNDERDAMPED REGIME $\chi \ll 1$

In the highly underdamped regime  $\chi \ll 1$ , the auxiliary functions are reduced to

$$h_\lambda^{\text{under}} = \frac{n+1}{2n\kappa\lambda} \left( \frac{1}{2m}p^2 + \frac{1}{2n}m\lambda^{n+1}x^{2n} \right), \quad (\text{S95})$$

$$h_\beta^{\text{under}} = \frac{n+1}{2n\kappa\beta} \left( \frac{1}{2m}p^2 + \frac{1}{2n}m\lambda^{n+1}x^{2n} \right). \quad (\text{S96})$$

The auxiliary Hamiltonian becomes

$$H_a^{\text{under}} = \frac{n+1}{2n\kappa} \left( \frac{\dot{\lambda}}{\lambda} + \frac{\dot{\beta}}{\beta} \right) \left( \frac{1}{2m}p^2 + \frac{1}{2n}m\lambda^{n+1}x^{2n} \right), \quad (\text{S97})$$

which is proportional to the original Hamiltonian. Therefore, an equilibrium state of the original Hamiltonian is also an equilibrium state of the total Hamiltonian with a different effective temperature  $T_{\text{eff}}^{\text{under}}$ , which is explicitly

$$T_{\text{eff}}^{\text{under}} = \left[ 1 + \frac{n+1}{2n\kappa} \left( \frac{\dot{\lambda}}{\lambda} + \frac{\dot{\beta}}{\beta} \right) \right] \frac{1}{\beta}. \quad (\text{S98})$$

The irreversible work and the thermodynamic length are dominated by the first term of Eqs. (S46) and (S47), and are explicitly

$$W_{\text{irr}}^{\text{under}} = \frac{(n+1)^2}{4n^2\kappa\beta} \int_0^\tau \left( \frac{\dot{\lambda}}{\lambda} + \frac{\dot{\beta}}{\beta} \right)^2 dt, \quad (\text{S99})$$

$$\mathcal{L}^{\text{under}} = \frac{n+1}{2n\sqrt{\kappa\beta}} \oint \left| \frac{\lambda'(s)}{\lambda} + \frac{\beta'(s)}{\beta} \right| ds. \quad (\text{S100})$$

It is worth noting that the expressions (S99) and (S100) depend on  $n$  through the effective degree of freedom  $f_n = 1 + 1/n$ . The auxiliary Hamiltonian (S97) is zero on the exponential paths with  $\alpha = 1$ , and the irreversible work and the thermodynamic length are also zero. The optimal connecting paths should be chosen as two of these exponential paths (IV)  $T = T_L \exp(r - r_1)$  and (II)  $T = T_L \exp(r - r_2)$  with zero thermodynamic lengths  $\mathcal{L}_{\text{IV}}^{\text{under}} = \mathcal{L}_{\text{II}}^{\text{under}} = 0$ , and the boundary values of the control parameters are related by

$$r'_1 = r_1 + \ln \left( \frac{T_H}{T_L} \right), \quad (\text{S101})$$

$$r'_2 = r_2 + \ln \left( \frac{T_H}{T_L} \right). \quad (\text{S102})$$

The quasistatic processes on these paths are adiabatic since  $\dot{Q}_o = 0$  [Eq. (S43)]. In the highly underdamped regime, the finite-time processes on these paths are also adiabatic, namely  $Q_{\text{IV}}^{\text{under}} = 0$  and  $Q_{\text{II}}^{\text{under}} = 0$ , since  $\dot{Q} = \dot{Q}_o + \dot{Q}_{\text{irr}} = 0$ .

The quasistatic heat of the two isothermal processes is obtained from Eq. (S43) as

$$Q_{o,\text{I}}^{\text{under}} = -\frac{n+1}{2n} \int_{r_1}^{r_2} T_L dr \quad (\text{S103})$$

$$= -\frac{n+1}{2n} T_L (r_2 - r_1), \quad (\text{S104})$$

and

$$Q_{o,\text{III}}^{\text{under}} = -\frac{n+1}{2n} \int_{r'_2}^{r'_1} T_H dr \quad (\text{S105})$$

$$= \frac{n+1}{2n} T_H (r_2 - r_1), \quad (\text{S106})$$

Since the connecting processes are adiabatic, the overall heat absorbed in a quasistatic cycle is  $Q_{o,+}^{\text{under}} = Q_{o,\text{III}}^{\text{under}}$ , and the overall heat released is  $Q_{o,-}^{\text{under}} = Q_{o,\text{I}}^{\text{under}}$ . The area of the closed path is

$$\mathcal{A}^{\text{under}} = (T_H - T_L)(r_2 - r_1), \quad (\text{S107})$$

and the quasistatic work of the cycle is

$$W_o^{\text{under}} = -\frac{n+1}{2n} (T_H - T_L)(r_2 - r_1). \quad (\text{S108})$$

The efficiency of the quasistatic cycle is the Carnot efficiency

$$\eta_o^{\text{under}} = -\frac{W_o^{\text{under}}}{Q_{o,+}^{\text{under}}} \quad (\text{S109})$$

$$= 1 - \frac{T_L}{T_H}. \quad (\text{S110})$$

The thermodynamic lengths (S63) and (S65) of the isothermal paths are simplified into

$$\mathcal{L}_I^{\text{under}} = \frac{n+1}{2n} \sqrt{\frac{T_L}{\kappa}} (r_2 - r_1), \quad (\text{S111})$$

and

$$\mathcal{L}_{III}^{\text{under}} = \frac{n+1}{2n} \sqrt{\frac{T_H}{\kappa}} (r_2 - r_1). \quad (\text{S112})$$

They satisfy the relation

$$\frac{\mathcal{L}_I^{\text{under}}}{\mathcal{L}_{III}^{\text{under}}} = \sqrt{\frac{T_L}{T_H}}. \quad (\text{S113})$$

The thermodynamic lengths of the heat absorbed path and the heat released path are  $\mathcal{L}_+^{\text{under}} = \mathcal{L}_{III}^{\text{under}}$  and  $\mathcal{L}_-^{\text{under}} = \mathcal{L}_I^{\text{under}}$ . The thermodynamic length of the whole cycle is

$$\mathcal{L}^{\text{under}} = \frac{n+1}{2n} \frac{\sqrt{T_L} + \sqrt{T_H}}{\sqrt{\kappa}} (r_2 - r_1). \quad (\text{S114})$$

The efficiency at the maximum power [Eq. (21) in the main text] is then obtained with the results of  $\eta_o^{\text{under}}$ ,  $\mathcal{L}_+^{\text{under}}$  and  $\mathcal{L}^{\text{under}}$ .

### A. Optimal protocol

The optimal protocol on the closed path is given by varying the control parameters with a constant velocity of the thermodynamic length, i.e.,

$$\frac{d\mathcal{L}}{ds} = \mathcal{L}^{\text{under}}, \quad (\text{S115})$$

where  $s \in [0, 1]$  is the rescaled time. The control scheme of the work parameter is given by

$$r^{\text{under}}(s) = \begin{cases} r_1 + (r_2 - r_1) \left(1 + \sqrt{\frac{T_H}{T_L}}\right) s & 0 < s < \frac{1}{1 + \sqrt{T_H/T_L}} \\ r'_2 + (r'_1 - r'_2) \left(1 + \sqrt{\frac{T_L}{T_H}}\right) \left(s - \frac{1}{1 + \sqrt{T_H/T_L}}\right) & \frac{1}{1 + \sqrt{T_H/T_L}} < s < 1 \end{cases}, \quad (\text{S116})$$

or

$$\lambda^{\text{under}}(s) = \begin{cases} \lambda_1 \left(\frac{\lambda_2}{\lambda_1}\right)^{(1 + \sqrt{T_H/T_L})s} & 0 < s < \frac{1}{1 + \sqrt{T_H/T_L}} \\ \lambda'_2 \left(\frac{\lambda'_1}{\lambda'_2}\right)^{(1 + \sqrt{T_L/T_H})s - \sqrt{T_L/T_H}} & \frac{1}{1 + \sqrt{T_H/T_L}} < s < 1 \end{cases}, \quad (\text{S117})$$

where  $\lambda_1 = \lambda_0 \exp(r_1)$ ,  $\lambda_2 = \lambda_0 \exp(r_2)$ ,  $\lambda'_1 = \lambda_0 \exp(r'_1)$  and  $\lambda'_2 = \lambda_0 \exp(r'_2)$ . The control scheme of the temperature is given by

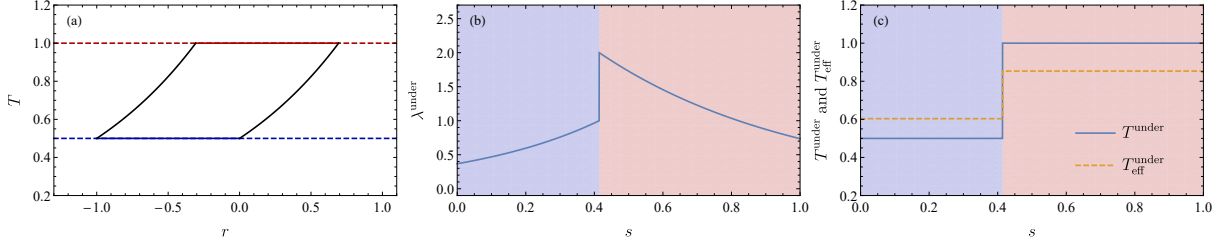


Figure S3. Optimal protocol in the highly underdamped regime. (a) The  $r - T$  diagram. (b) The optimal protocol to vary the frequency  $\lambda^{\text{under}}(s)$ . (c) The evolution of the temperatures.

$$T^{\text{under}}(s) = \begin{cases} T_L & 0 < s < \frac{1}{1 + \sqrt{T_H/T_L}} \\ T_H & \frac{1}{1 + \sqrt{T_H/T_L}} < s < 1 \end{cases}. \quad (\text{S118})$$

It is worth noting that the optimal protocol in the highly underdamped regime does not depend on the shape of the potential  $n$ .

The evolution of the effective temperature in a cycle according to Eq. (S98) is

$$T_{\text{eff}}^{\text{under}}(s) = \begin{cases} T_L \left[ 1 + \frac{n+1}{2n\kappa\tau} \left( 1 + \sqrt{T_H/T_L} \right) \ln(\lambda_2/\lambda_1) \right] & 0 < s < \frac{1}{1 + \sqrt{T_H/T_L}} \\ T_H \left[ 1 + \frac{n+1}{2n\kappa\tau} \left( 1 + \sqrt{T_L/T_H} \right) \ln(\lambda'_1/\lambda'_2) \right] & \frac{1}{1 + \sqrt{T_H/T_L}} < s < 1 \end{cases}. \quad (\text{S119})$$

The operation time consumed in each process, according to Eq. (S76), is

$$\tau_{\text{I}}^{\text{under}} = \frac{\sqrt{T_L}}{\sqrt{T_L} + \sqrt{T_H}} \tau \quad (\text{S120})$$

$$\tau_{\text{II}}^{\text{under}} = 0 \quad (\text{S121})$$

$$\tau_{\text{III}}^{\text{under}} = \frac{\sqrt{T_H}}{\sqrt{T_L} + \sqrt{T_H}} \tau \quad (\text{S122})$$

$$\tau_{\text{IV}}^{\text{under}} = 0. \quad (\text{S123})$$

Compared to the isothermal processes I and III, the connecting processes II and IV consume negligible time.

Figure S3 shows the optimal protocol of the cycle in the highly underdamped regime. We consider the harmonic potential  $n = 1$  here. Figure S3(a) is the  $r - T$  diagram of the cycle. The boundary values of the frequency on the low-temperature line  $T = T_L = 1/2$  are  $\lambda_1 = 1/e$ ,  $\lambda_2 = 1$  with  $e = 2.718$ . These parameters are the same with those in the main text. The boundary values of the frequency on the high-temperature line  $T = T_H = 1$  are  $\lambda'_1 = \lambda_1 T_H/T_L = 2/e$  and  $\lambda'_2 = \lambda_2 T_H/T_L = 2$ . The friction coefficient is set to be  $\kappa = 0.1$ . The area of the closed path is  $\mathcal{A}^{\text{under}} = 1/2$ , and the thermodynamic length of the cycle is  $\mathcal{L}^{\text{under}} = 5.40$ . We set the operation time of the cycle to be  $\tau_{\text{max}}^{\text{under}} = 116.57$  to reach the maximum output power  $P_{\text{max}}^{\text{under}} = 0.0021$ . Figure S3(b) shows the optimal protocol (S117) to vary the frequency  $\lambda^{\text{under}}(s)$  in a cycle. Figure S3(c) shows the evolution of the temperatures in a cycle. The effective temperature  $T_{\text{eff}}^{\text{under}}$  defined by Eq. (S119) remain unchanged during the isothermal processes.

## B. Comparison to Refs. [7, 8]

In the shortcut strategy, we need to implement the auxiliary Hamiltonian  $H_a$  [Eq. (S97)]. The moment term in  $H_a$  changes the mass of the particle. Notice that in Refs. [7, 8] only the potential can be varied in the isothermal processes, not the mass of the particle. As a result, the optimal protocol (S117) is not exactly the same as the one

obtained in Refs. [7, 8]. The ratio of the time consumed in the two isothermal process is  $\tau_I^{\text{under}}/\tau_{III}^{\text{under}} = \sqrt{T_L/T_H}$ , while the ratio is equal to one in the protocol of Refs. [7, 8]. It is the same reason that the maximum power at given efficiency [Eq. (S92)] is different from the one (S93) obtained in Refs. [6–8].

We continue to compare the expressions of the output power in this work and the one obtained in [8]. In this work, the output power according to Eq. (S79) is bounded by

$$P^{\text{under}} \leq \frac{n+1}{2n} (T_H - T_L)(r_2 - r_1) \frac{1}{\tau} - \left[ \frac{n+1}{2n} \frac{\sqrt{T_L} + \sqrt{T_H}}{\sqrt{\kappa}} (r_2 - r_1) \right]^2 \frac{1}{\tau^2}. \quad (\text{S124})$$

The irreversible work of the cycle is rigorously proportional to the inverse of the operation time. In Ref. [8], we have also obtained the bound of the output power [see Eq. (13) of Ref. [8]], which in the current notation is explicitly

$$\tilde{P}^{\text{under}} \leq \frac{\kappa}{2} \left( \frac{T_H}{\frac{\tau}{2} \frac{2n}{n+1} \frac{\kappa}{(r_2-r_1)} + 1} - \frac{T_L}{\frac{\tau}{2} \frac{2n}{n+1} \frac{\kappa}{(r_2-r_1)} - 1} \right), \quad (\text{S125})$$

We have substituted the parameters  $\Gamma_H$ ,  $\Gamma_C$ ,  $\tau_H$ ,  $\tau_C$ ,  $r$ ,  $T_C$  in Ref. [8] with the current parameters

$$\Gamma_H = \Gamma_C \rightarrow \frac{2n}{n+1} \kappa \quad (\text{S126})$$

$$\tau_H = \tau_C \rightarrow \frac{\tau}{2} \quad (\text{S127})$$

$$\ln r \rightarrow r_2 - r_1 \quad (\text{S128})$$

$$T_C \rightarrow T_L. \quad (\text{S129})$$

One can see that the expressions (S124) and (S125) are different, but share the same maximum value  $P_{\text{max}}^{\text{under}} = \kappa(\sqrt{T_H} - \sqrt{T_L})^2/4$  by choosing a proper value of the operation time  $\tau$ .

## VII. OVERDAMPED REGIME $\chi \gg 1$

In the overdamped regime  $\chi \gg 1$ , the auxiliary functions are reduced to

$$h_\lambda^{\text{over}} = \frac{n+1}{4n\lambda} \kappa m x^2, \quad (\text{S130})$$

$$h_\beta^{\text{over}} = \frac{1}{4n\beta} \kappa m x^2. \quad (\text{S131})$$

The auxiliary Hamiltonian becomes

$$H_a^{\text{over}} = \frac{\kappa m}{4n} \left[ (n+1) \frac{\dot{\lambda}}{\lambda} + \frac{\dot{\beta}}{\beta} \right] x^2, \quad (\text{S132})$$

which is just a harmonic potential of the position.

The irreversible work and the thermodynamic length are dominated by the second term of Eqs. (S46) and (S47), and are explicitly

$$W_{\text{irr}}^{\text{over}} = \frac{(n+1)^2}{4n^2} \int_0^\tau \frac{\kappa m}{\lambda} \frac{R_n}{(\lambda m \beta)^{1/n}} \left( \frac{\dot{\lambda}}{\lambda} + \frac{\dot{\beta}}{(n+1)\beta} \right)^2 dt, \quad (\text{S133})$$

$$\mathcal{L}^{\text{over}} = \frac{n+1}{2n} \oint \sqrt{\frac{\kappa m}{\lambda} \frac{R_n}{(\lambda m \beta)^{1/n}}} \left| \frac{\lambda'(s)}{\lambda} + \frac{\beta'(s)}{(n+1)\beta} \right| ds. \quad (\text{S134})$$

On the exponential paths with  $\alpha = n+1$ , the auxiliary Hamiltonian (S132) is zero, and the irreversible work and the thermodynamic length are also zero. The optimal connecting paths should be chosen as two of these exponential



paths (IV)  $T = T_L \exp[(n+1)(r-r_1)]$  and (II)  $T = T_L \exp[(n+1)(r-r_2)]$  with zero thermodynamic lengths  $\mathcal{L}_{\text{IV}}^{\text{over}} = \mathcal{L}_{\text{II}}^{\text{over}} = 0$ , and the boundary values of the control parameters are related by

$$r'_1 = r_1 + \frac{1}{n+1} \ln \left( \frac{T_H}{T_L} \right), \quad (\text{S135})$$

$$r'_2 = r_2 + \frac{1}{n+1} \ln \left( \frac{T_H}{T_L} \right). \quad (\text{S136})$$

We calculate the quasistatic heat of each process according to Eq. (S43). The quasistatic heat of the two connecting processes is

$$Q_{\text{o,II}}^{\text{over}} = \frac{n+1}{2} \int_{r_2}^{r'_2} T_L \exp[(n+1)(r-r_2)] dr \quad (\text{S137})$$

$$= \frac{1}{2} (T_H - T_L), \quad (\text{S138})$$

and

$$Q_{\text{o,IV}}^{\text{over}} = -\frac{1}{2} (T_H - T_L). \quad (\text{S139})$$

The heat  $Q_{\text{o,II}}^{\text{over}}$  and  $Q_{\text{o,IV}}^{\text{over}}$  are equal to the change of the kinetic energy at two temperatures  $T_L$  and  $T_H$ . In a whole cycle, besides the heat generated in the isothermal processes, additional heat  $(T_H - T_L)/2$  is transferred from the hot bath to the cold bath. This additional heat is the heat leakage [5]. The quasistatic heat of the two isothermal processes is

$$Q_{\text{o,I}}^{\text{over}} = -\frac{n+1}{2n} T_L (r_2 - r_1), \quad (\text{S140})$$

and

$$Q_{\text{o,III}}^{\text{over}} = \frac{n+1}{2n} T_H (r_2 - r_1). \quad (\text{S141})$$

In a quasistatic cycle, the overall heat absorbed is

$$Q_{\text{o,+}}^{\text{over}} = Q_{\text{o,III}}^{\text{over}} + Q_{\text{o,II}}^{\text{over}} \quad (\text{S142})$$

$$= \frac{n+1}{2n} T_H (r_2 - r_1) + \frac{1}{2} (T_H - T_L) \quad (\text{S143})$$

and the overall heat released is

$$Q_{\text{o,-}}^{\text{over}} = Q_{\text{o,I}}^{\text{over}} + Q_{\text{o,IV}}^{\text{over}} \quad (\text{S144})$$

$$= -\frac{n+1}{2n} T_L (r_2 - r_1) - \frac{1}{2} (T_H - T_L). \quad (\text{S145})$$

The area of the closed path is

$$\mathcal{A}^{\text{over}} = (T_H - T_L) (r_2 - r_1), \quad (\text{S146})$$

and the quasistatic work of the cycle is

$$W_{\text{o}}^{\text{over}} = -\frac{n+1}{2n} (T_H - T_L) (r_2 - r_1). \quad (\text{S147})$$

The quasistatic efficiency is

$$\eta_o^{\text{over}} = -\frac{W_o^{\text{over}}}{Q_{o,+}^{\text{over}}} \quad (\text{S148})$$

$$= \frac{\eta_C}{1 + \frac{n}{n+1} \frac{\eta_C}{(r_2 - r_1)}}. \quad (\text{S149})$$

The thermodynamic lengths (S63) and (S65) of the isothermal paths are simplified into

$$\mathcal{L}_I^{\text{over}} = \sqrt{R_n \frac{\kappa m}{\lambda_0} \left( \frac{T_L}{\lambda_0 m} \right)^{1/n}} \left( e^{-\frac{(n+1)}{2n} r_1} - e^{-\frac{(n+1)}{2n} r_2} \right), \quad (\text{S150})$$

and

$$\mathcal{L}_{III}^{\text{over}} = \sqrt{R_n \frac{\kappa m}{\lambda_0} \left( \frac{T_H}{\lambda_0 m} \right)^{1/n}} \left( e^{-\frac{(n+1)}{2n} r'_1} - e^{-\frac{(n+1)}{2n} r'_2} \right). \quad (\text{S151})$$

The two thermodynamic lengths are equal  $\mathcal{L}_{III}^{\text{over}} = \mathcal{L}_I^{\text{over}}$  by plugging Eqs. (S135) and (S136) into Eq. (S151). Thus, in the overdamped regime, the two isothermal processes consume the same operation time in the optimal cycle. Since the thermodynamic lengths of the connecting paths are zero, the thermodynamic lengths of the heat absorbed path and the heat released path are  $\mathcal{L}_+^{\text{over}} = \mathcal{L}_{III}^{\text{over}}$  and  $\mathcal{L}_-^{\text{over}} = \mathcal{L}_I^{\text{over}}$ . The thermodynamic length of the whole cycle is

$$\mathcal{L}^{\text{over}} = 2\sqrt{R_n \frac{\kappa m}{\lambda_0} \left( \frac{T_L}{\lambda_0 m} \right)^{1/n}} \left( e^{-\frac{(n+1)}{2n} r_1} - e^{-\frac{(n+1)}{2n} r_2} \right). \quad (\text{S152})$$

The efficiency at the maximum power [Eq. (26) in the main text] is then obtained with the results of  $\eta_o^{\text{over}}$ ,  $\mathcal{L}_+^{\text{over}}$  and  $\mathcal{L}^{\text{over}}$ .

### A. Optimal protocol

The optimal protocol is solved from

$$\frac{d\mathcal{L}}{ds} = \mathcal{L}^{\text{over}}. \quad (\text{S153})$$

We plug the expressions (S150) and (S151) into Eq. (S153), and obtain the control scheme of the work parameter

$$r^{\text{over}}(s) = \begin{cases} -\frac{2n}{n+1} \ln[(1-2s)e^{-\frac{(n+1)}{2n} r_1} + 2se^{-\frac{(n+1)}{2n} r_2}] & 0 < s < \frac{1}{2} \\ -\frac{2n}{n+1} \ln[(2-2s)e^{-\frac{(n+1)}{2n} r'_2} + (2s-1)e^{-\frac{(n+1)}{2n} r'_1}] & \frac{1}{2} < s < 1 \end{cases}, \quad (\text{S154})$$

or

$$\lambda^{\text{over}}(s) = \begin{cases} \left[ (1-2s)\lambda_1^{-\frac{(n+1)}{2n}} + 2s\lambda_2^{-\frac{(n+1)}{2n}} \right]^{-\frac{2n}{n+1}} & 0 < s < \frac{1}{2} \\ \left[ (2-2s)\lambda_2'^{-\frac{(n+1)}{2n}} + (2s-1)\lambda_1'^{-\frac{(n+1)}{2n}} \right]^{-\frac{2n}{n+1}} & \frac{1}{2} < s < 1 \end{cases}. \quad (\text{S155})$$

The control scheme of the temperature is given by

$$T^{\text{over}}(s) = \begin{cases} T_L & 0 < s < \frac{1}{2} \\ T_H & \frac{1}{2} < s < 1 \end{cases}. \quad (\text{S156})$$

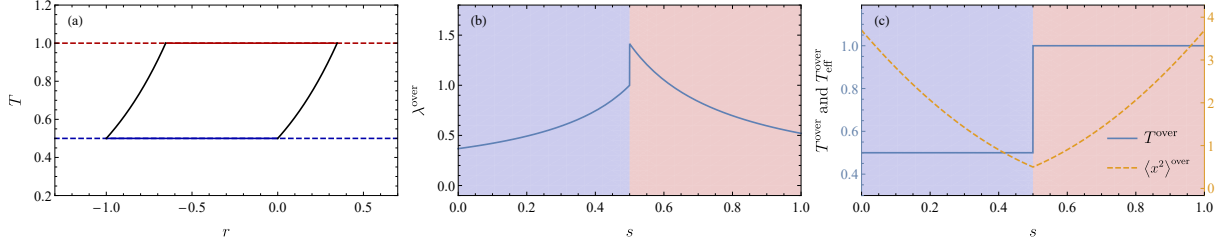


Figure S4. Optimal protocol in the overdamped regime. (a) The  $r-T$  diagram. (b) The optimal protocol to vary the frequency  $\lambda^{\text{over}}(s)$ . (c) The evolution of the temperatures.

The variance of position in a cycle according to Eq. (S35) is

$$\langle x^2 \rangle^{\text{over}}(s) = \begin{cases} R_n \left(\frac{T_L}{m}\right)^{1/n} \left[ (1-2s)\lambda_1^{-\frac{(n+1)}{2n}} + 2s\lambda_2^{-\frac{(n+1)}{2n}} \right]^2 & 0 < s < \frac{1}{2} \\ R_n \left(\frac{T_H}{m}\right)^{1/n} \left[ (2-2s)\lambda_2'^{-\frac{(n+1)}{2n}} + (2s-1)\lambda_1'^{-\frac{(n+1)}{2n}} \right]^2 & \frac{1}{2} < s < 1 \end{cases}. \quad (\text{S157})$$

It can be verified that  $\langle x^2 \rangle^{\text{over}}(s)$  is continuous at the piecewise points  $s = 0$  and  $s = 1/2$ . In the two connecting processes, the control parameters are switched suddenly. The distribution of the momentum changes to the equilibrium state at the new temperature, while the distribution of the coordinate remains unchanged.

Figure S4 shows the optimal protocol of the cycle in the overdamped regime. We still consider the harmonic potential  $n = 1$ . Figure S4(a) is the  $r-T$  diagram of the cycle. The boundary values of the frequency on the low-temperature line  $T = T_L = 1/2$  are  $\lambda_1 = 1/e$ ,  $\lambda_2 = 1$  with  $e = 2.718$ . The boundary values of the frequency on the high-temperature line  $T = T_H = 1$  are  $\lambda_1' = \lambda_1 \sqrt{T_H/T_L} = \sqrt{2}/e$  and  $\lambda_2' = \lambda_2 \sqrt{T_H/T_L} = \sqrt{2}$ . The friction coefficient is set to be  $\kappa = 10$  for the overdamped regime. The area of the closed path is  $\mathcal{A}^{\text{over}} = 1/2$ , and the thermodynamic length of the cycle is  $\mathcal{L}^{\text{over}} = 7.68$ . We set the operation time of the cycle  $\tau_{\text{max}}^{\text{over}} = 236.20$  to reach the maximum output power  $P_{\text{max}}^{\text{over}} = 0.0011$ . Figure S4(b) shows the optimal protocol (S160) to vary the frequency  $\lambda^{\text{over}}(s)$  in a cycle. Figure S4(c) shows the evolution of the temperature  $T^{\text{over}}(s)$  and the variance of the position  $\langle x^2 \rangle^{\text{over}}(s)$  in a cycle.

## B. Comparison to Ref. [5]

For the harmonic potential  $n = 1$ , the auxiliary Hamiltonian (S132) is explicitly

$$H_a^{\text{over}} = \frac{1}{2} m \kappa \left( \frac{\dot{\lambda}}{\lambda} + \frac{\dot{\beta}}{2\beta} \right) x^2. \quad (\text{S158})$$

The implementation of the auxiliary Hamiltonian is equivalent to changing the frequency of the harmonic potential into

$$\Lambda^{\text{over}} = \sqrt{\lambda^2 + \kappa \left( \frac{\dot{\lambda}}{\lambda} + \frac{\dot{\beta}}{2\beta} \right)}. \quad (\text{S159})$$

Therefore, the optimal protocol with the shortcut strategy in the overdamped regime converges to the control scheme obtained in Ref. [5]. The control scheme (S155) to vary the work parameter is explicitly

$$\lambda^{\text{over}}(s) = \begin{cases} \frac{\lambda_1}{1-2s+2s\lambda_1/\lambda_2} & 0 < s < \frac{1}{2} \\ \frac{\lambda_2'}{2-2s+(2s-1)\lambda_2'/\lambda_1'} & \frac{1}{2} < s < 1 \end{cases}, \quad (\text{S160})$$

The variance of the particle position  $\langle x^2 \rangle$  is explicitly

$$\langle x^2 \rangle^{\text{over}}(s) = \begin{cases} \frac{T_L}{\lambda_1^2 m} (1 - 2s + 2s\lambda_1/\lambda_2)^2 & 0 < s < \frac{1}{2} \\ \frac{T_H}{\lambda_2^2 m} [2 - 2s + (2s - 1)\lambda_2'/\lambda_1']^2 & \frac{1}{2} < s < 1 \end{cases}, \quad (\text{S161})$$

which is the same as the result obtained in Ref. [5].

An effective temperature of the position degree of freedom can be defined in respective to the altered frequency

$$T_{\text{eff}}^{\text{over}} := m(\Lambda^{\text{over}})^2 \langle x^2 \rangle^{\text{over}}. \quad (\text{S162})$$

Its evolution in a cycle is

$$T_{\text{eff}}^{\text{over}}(s) = \begin{cases} \left[ 1 - \frac{2\kappa}{\lambda_1^2 \lambda_2^2 \tau} (\lambda_1 - \lambda_2) [\lambda_2 + 2(\lambda_1 - \lambda_2)s] \right] T_L & 0 < s < \frac{1}{2} \\ \left[ 1 + \frac{2\kappa}{\lambda_1'^2 \lambda_2'^2 \tau} (\lambda_1' - \lambda_2') [2\lambda_1' - \lambda_2' + 2(\lambda_2' - \lambda_1')s] \right] T_H & \frac{1}{2} < s < 1 \end{cases}, \quad (\text{S163})$$

which is not a constant during the isothermal processes.

---

\* [chenjinfu@pku.edu.cn](mailto:chenjinfu@pku.edu.cn)

- [1] G. Li, H. T. Quan, and Z. C. Tu, Shortcuts to isothermality and nonequilibrium work relations, *Phys. Rev. E* **96**, 012144 (2017).
- [2] Y. Jun and P.-Y. Lai, Instantaneous equilibrium transition for Brownian systems under time-dependent temperature and potential variations: Reversibility, heat and work relations, and fast isentropic process, *Phys. Rev. Research* **3**, 033130 (2021).
- [3] M. Berger, *A Panoramic View of Riemannian Geometry* (Springer Berlin Heidelberg, 2007).
- [4] F. L. Curzon and B. Ahlborn, Efficiency of a Carnot engine at maximum power output, *Am. J. Phys.* **43**, 22 (1975).
- [5] T. Schmiedl and U. Seifert, Efficiency at maximum power: An analytically solvable model for stochastic heat engines, *Europhys. Lett.* **81**, 20003 (2007).
- [6] L. Chen and Z. Yan, The effect of heat-transfer law on performance of a two-heat-source endoreversible cycle, *J. Chem. Phys.* **90**, 3740 (1989).
- [7] A. Dechant, N. Kiesel, and E. Lutz, Underdamped stochastic heat engine at maximum efficiency, *Europhys. Lett.* **119**, 50003 (2017).
- [8] Y. H. Chen, J.-F. Chen, Z. Fei, and H. T. Quan, A microscopic theory of Curzon-Ahlborn heat engine, (2021), [arXiv:2108.04128v2](https://arxiv.org/abs/2108.04128v2) [cond-mat.stat-mech].